5-1-2009

Characterization of tissue mimicking materials for testing of implantable and on body antennas

Tuba Yilmaz

CHARACTERIZATION OF TISSUE MIMICKING MATERIALS FOR TESTING OF IMPLANTABLE AND ON BODY ANTENNAS

By

Tuba Yilmaz

A Thesis
Submitted to the Faculty of
Mississippi State University
in Partial Fulfillment of the Requirements
for the Degree of Master of Science
in Electrical and Computer Engineering
in the Department of Electrical and Computer Engineering

Mississippi State, Mississippi

August 2009

CHARACTERIZATION OF TISSUE MIMICKING MATERIALS FOR TESTING OF IMPLANTABLE AND ON BODY ANTENNAS

By

Tuba Yilmaz

Approved:

Erdem Topsakal Associate Professor of Electrical and Computer Engineering (Director of Thesis)	J. Patrick Donohoe Professor of Electrical and Computer Engineering (Committee Member)
Burak Eksioglu Assistant Professor of Industrial and Systems Engineering (Committee Member)	James E. Fowler Professor of Electrical and Computer Engineering (Graduate Coordinator)

Sarah A. Rajala
Dean of the Bagley College of Engineering

Name: Tuba Yilmaz

Date of Degree: August 8, 2009

Major Field: Electrical and Computer Engineering

Major Professor: Dr. Erdem Topsakal

Title of Study: CHARACTERIZATION OF TISSUE MIMICKING MATERIALS FOR TESTING OF IMPLANTABLE AND ON-BODY ANTENNAS

Pages in Study: 56

Candidate for Degree of Master and Science

Characterization and applications of soft tissue mimicking materials are presented. A skin mimicking material and a skin mimicking gel is characterized for industrial, scientific, and medical (ISM) band (2.40 GHz-2.48 GHz). Also a wide band (0.3 GHz – 2.5 GHz) muscle mimicking material is developed. A dual band implantable antenna operating at medical implant communication service (MICS) band (402 MHz – 405 MHz) and ISM band is tested *in vitro* with skin mimicking material for ISM band. MICS band measurements of the implantable antenna tested *in vitro* by placing the antenna on the interface of muscle and skin mimicking gel. An on-body antenna operating at ISM Band is designed for wireless cardiac monitoring applications. The mutual coupling between the antennas is minimized by placing antennas with 90 degree phase difference. The recipes for tissue mimicking materials and results such as, comparison of electrical properties, return loss, and mutual coupling measurements is given.

DEDICATION

To my mother *Nurcan*

ACKNOWLEDGEMENTS

I would like to express my sincere gratitude to my advisor Dr. Erdem Topsakal for his constant support and guidance throughout the course of my research. I also thank him for having confidence in me and encouraging me through his passion on science.

I would like to thank Dr. Burak Eksioglu and Dr. J. Patrick Donohoe for their valuable time and for serving on my committee.

I would also like to thank many friends from Mississippi State University and my colleagues from ICARE lab Tutku Karacolak and Santosh Seran that have been valuable friends and supported me trough the past two years. Special thanks to Tugce Gizem Martagan for being a true sister to me and for all her valuable support. You were always there whenever I needed and Tugce, you are a true inspiration on my life. I am deeply indebted to you for your support, love, and encouragement.

Thank you grandpa Keramettin, your support and dedication helped me to be the person I am now. Special thanks to my grandmother and my aunt for being very hard working, dedicated, and passionate role models. I also want to express my deepest gratitude to my uncle for inspiring me with his work and personality from early age.

To my dearest parents, thank you for your endless support and unadulterated love. Mother, you always helped me to get through hard times, you made my life easier and you gave all your passion, love, compassion to me. Thank you for being the best mother ever. Father, I have been inspired from your courage and compassion. You encouraged

me to discover and share from very early age. Both of your teachings and values will always stay with me. Thank you, for all you have done for me.

TABLE OF CONTENTS

LIST OF TABLES

LIST OF FIGURES

FIGURE Page

FIGURE Page

FIGURE Page

CHAPTER I

INTRODUCTION

1.1 Overview

Recently demand for tissue mimicking phantoms is increased due to the need to develop, optimize, and test the medical equipments such as implantable devices, body-centric antennas, cardiac pacemakers, microwave imaging systems, and ultrasound equipments [1]-[3]. Testing of such devices in humans is a very challenging task which requires facilities and subject to strict regulations enforced by Food and Drug Administration (FDA). Thus, many applications regarding antenna and RF equipments were developed and tested with saline or similar body fluid equivalent solutions [2]. Characterizing materials that mimics the electrical properties of human tissues is a key component to guarantee the proper functioning of such equipments.

To obtain physically realistic body equivalent models, the tissue simulating materials should be in solid form, approximate the electrical properties of the intended tissues, and should not be interact with one another. Tissue mimicking phantoms are also required to simulate the size and shape of the mimicked human tissues which requires using multiple tissues. In addition, precise measurement techniques should be employed during the electrical property measurement. The purpose of this thesis is to introduce the soft tissue

equivalent materials such as skin, muscle and fat tissues and discuss the potential applications.

1.2 Thesis Organization

This thesis is organized in the following order,

Recipes of characterized tissue simulating materials are given in chapter II. In section 2.2, the skin mimicking material is proposed for ISM Band. The detailed recipe for the skin mimicking material and the procedure to compose the material is explained. Electrical property measurement results for the tissue simulating material are also given. Skin mimicking gel is proposed in section 2.3. A comparison between the electrical properties of skin mimicking gel and reference data [4]-[5] is given. A recipe for muscle mimicking gel and measurement results is given in section 2.4.

Chapter III discusses the potential applications of the proposed tissue mimicking materials. The design and testing of serpentine shaped dual band implantable antenna is discussed in section 3.2 and section 3.3. The antenna is designed with finite element boundary integral techniques and optimized by employing particle swarm optimization algorithm [6]. HFSS software is used to design the antenna. Antenna fabricated, embedded into the skin mimicking material proposed in section 2.2 and tested *in vitro*. The measurement and simulation results regarding return loss and gain of the antenna is given. In section 3.3, return loss measurement results of the implantable antenna with skin mimicking gel is proposed. The effect of the tissues lying beneath the antenna to return loss measurement is investigated by placing the implantable antenna in two layered

tissue model. The measurement results are given in section 3.3. In addition, body centric antennas operating at ISM band and the mutual coupling measurements of those antennas with tissue simulating materials is given in section 3.5.

Chapter VI concludes the thesis, briefly summarizes the results, and discusses the potential applications, further research on tissue simulating materials. In section 4.2, testing of implantable antenna with three layered tissue mimicking material is illustrated. For precise measurement results, mutual coupling measurements will be performed with tissue mimicking material covered mannequin torso, this concept is also given in section 4.2.

CHAPTER II

CHARACTERIZATION OF TISSUE MIMICKING MATERIALS

2.1 Motivation

Applications of electromagnetics in medicine have an increasing importance with the inventions of new techniques and equipments. To verify the proper functioning of newly developed equipments human or animal subjects such as rats, rabbits, and dogs can be used. However, using human subjects is subject to very strict regulations from Food and Drug Administration (FDA). Using animal subjects, on the other hand, is very costly and requires facilities that many institution do not have. The logical route to follow is to use tissue simulating materials in the design process of such devices, than using animal subjects, and finally after meeting the safety assessment requirements testing devices on humans. In this study, materials that mimics the dielectric constant (ε_r) and conductivity (σ) of human tissues are proposed. To this end, soft tissue simulating materials (skin and muscle) is presented in this chapter.

2.2 Characterization of Skin Mimicking Material for Industrial, Scientific, and Medical (ISM) (2.40 GHz – 2.48 GHz) Band

A skin mimicking material is characterized by mixing diethylene glycol butyl ether (DGBE), polyethylene glycol mono phenyl ether (Triton X-100), and de-ionized water.

First, the electrical properties of each ingredient were measured. Fig. 2.1 and Fig. 2.2 show the relative dielectric constant and conductivity measurements respectively, for pure Triton X-100, DGBE, and de-ionized water, respectively. Both DGBE and Triton X-100 have low relative dielectric constant and low electrical conductivity, especially at high frequencies. Triton X-100 decreases the relative dielectric constant and the conductivity of the de-ionized water, however, pure Triton X-100 is not solvable in de-ionized water [7]. Adding DGBE to Triton X-100 decreases the viscosity of ingredient and enables Triton X-100 to well mix with the water. Table 2.1 shows the concentrations of various ingredients used to construct the proposed skin mimicking material.

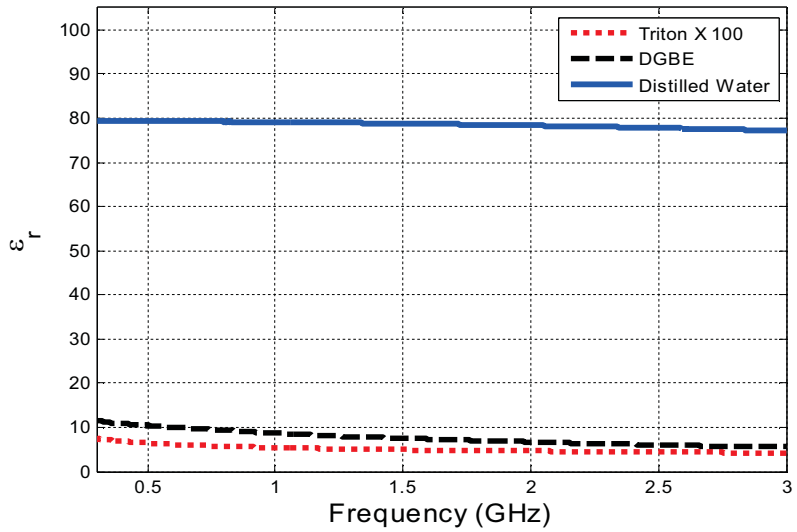

Fig. 2.1 Relative dielectric permittivity comparison of pure Triton X-100, DGBE, and Distilled Water.

It is important to mix the ingredients in proper order. First, Triton X-100 and DGBE is mixed and as the viscosity of the Triton X-100 decreased, de-ionized water is added slowly to the mixture by string the mixture tardily and with avoiding air bubbles.

Obtaining a mixture without air bubbles is vital to obtain accurate electrical property measurements.

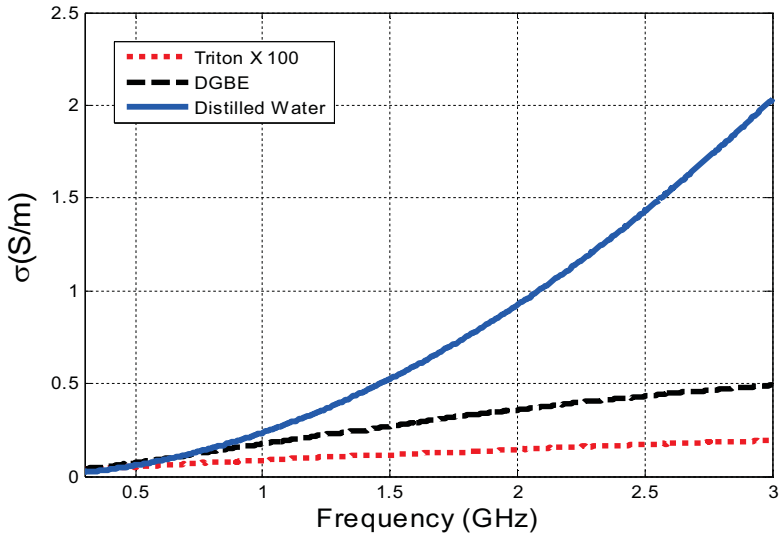

Fig. 2.2 Conductivity comparison of pure Triton X-100, DGBE, and Distilled Water.

Table 2.1

Recipe for Skin Mimicking Material

	ISM (2.40GHz – 2.48 GHz)Band
De-ionized Water	58.2%
Triton X-100	36.7%
DGBE	5.1%

Fig. 2.3 shows a very simple process to characterize proposed skin mimicking Material with using few ingredients in a short period of time. It is important to propose a simple recipe for characterization of such materials to minimize measurement error originated from chemicals and to reduce the cost.

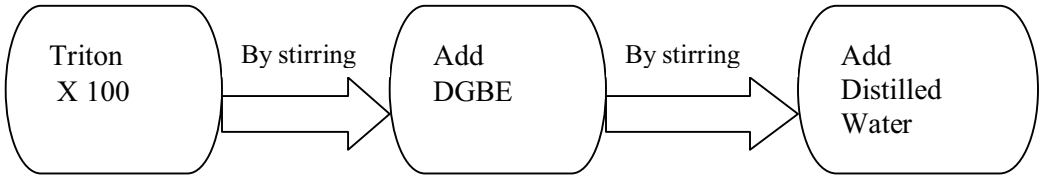

Fig. 2.3. Process of preparing skin mimicking material.

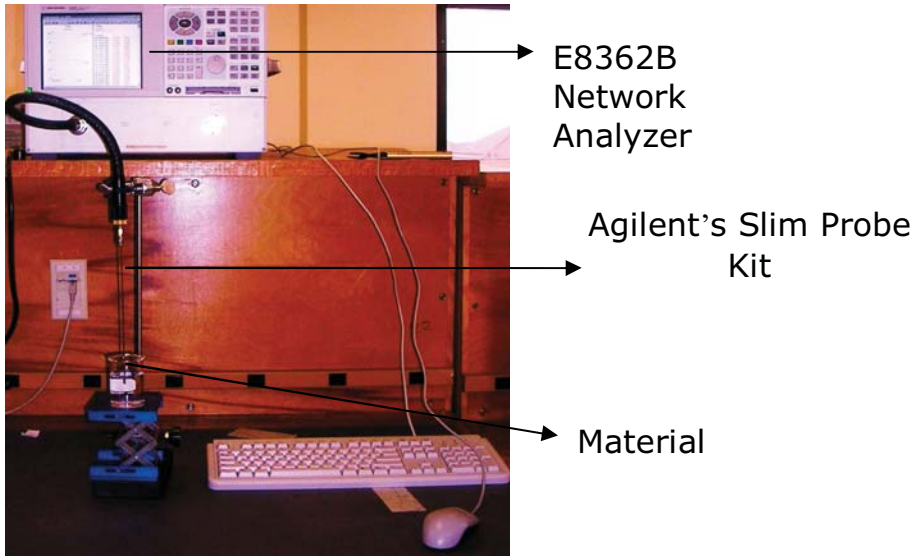

Fig. 2.4 Measurement set-up for electrical property measurements.

Experiment set up for electrical property measurements is demonstrated with Fig. 2.4. Note that all measurements performed with E8362B network analyzer and Agilent's slim probe kit.

Characterized skin mimicking material's electrical properties is measured from 300 MHz to 3.0 GHz. Obtained measurements are compared with the reference data obtained from Gabriel et al [4]-[5]. In [4] a comprehensive literature survey of previously measured electrical properties of different tissues either excited from human body or

excited from animals is provided. In [5] the electrical property measurements of different tissues from 10 Hz to 20 GHz are given. The measurements are taken from (i) excised animal tissue, mostly ovine, some porcine, from freshly killed animals; (ii) human autopsy materials and (iii) human skin and tongue in vivo. The animal tissue measurements mostly measured after 2 h of the animal's death; human materials are obtained 24 to 48 hours after death. The genders or ages of the animal or human subjects aren't specified in the reference. The temperature and moisture of the materials during measurement is not specifies. In [5] a comparison between in vivo and in vitro electrical property measurements is given. Also the reference obtained a good agreement between the data available in literature and measurements. In this paper the measurements are compared with the dry skin data in Gabriel et al.

A good agreement is obtained between reference data in [4]-[5] and measurements for ISM Band. Graphical comparison between relative permittivity and conductivity of measured and reference data in [4]-[5] is given in Fig. 2.5 and Fig. 2.6 respectively.

At 2.4 GHz, the conductivity of the skin mimicking material (σ= 1.4421) matches very well with the reference data (σ=1.4407) in [4]-[5]. The relative dielectric constant of the skin mimicking material is 37.884, which is slightly lower than the relative dielectric constant of the reference data (38.063) in [4]-[5]. Estimated errors for both ε_r and σ are given in (1) and (2) for the entire ISM band.

Calculated maximum error in the 2.4 GHz – 2.48 GHz band is

$$Error_{\varepsilon_r} = \frac{|\varepsilon_{r(material)} - \varepsilon_{r(human)}|}{\varepsilon_{r(human)}} < 0.5\% \quad (1)$$

for the relative dielectric constant and

$$Error_{\sigma} = \frac{|\sigma_{human} - \sigma_{material}|}{\sigma_{human}} < 3.4\% \quad (2)$$

for conductivity.

The advantages of proposed skin mimicking material can be summarized as follows;

- contains very few ingredients
- doesn't requires elaborated steps and expensive facilities to be characterized
- composition of the material is not a costly
- requires a simple procedure.

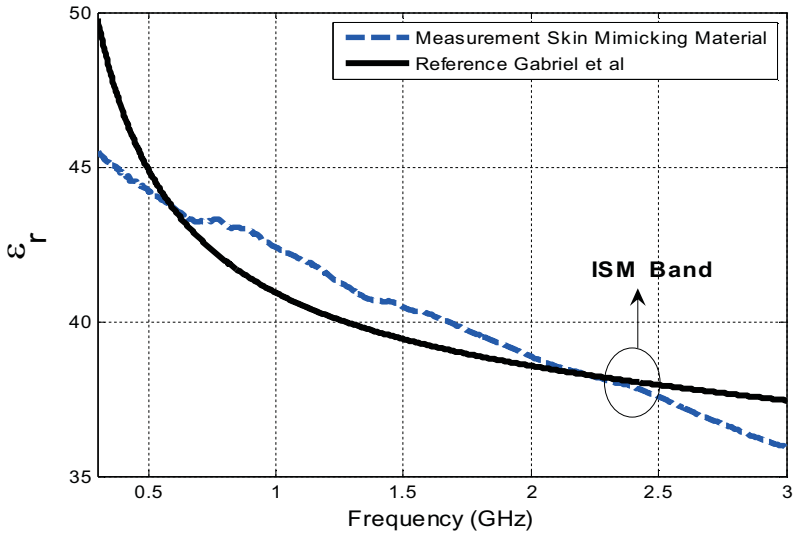

Fig. 2.5 Relative dielectric permittivity comparison of characterized tissue mimicking material and reference data in [4]-[5].

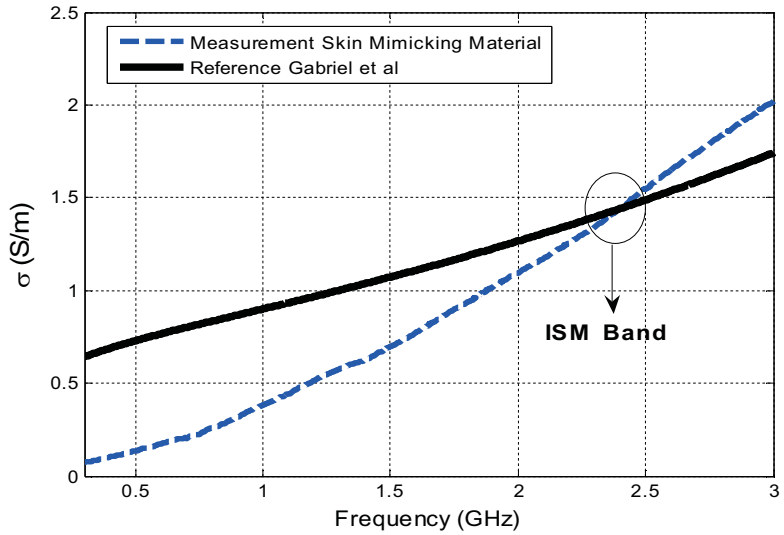

Fig. 2.6 Conductivity comparison of characterized tissue mimicking material and reference data in [4]-[5].

Electrical properties of the material are matched with real human skin very well for ISM band and the material can be used to investigate the interaction between the electromagnetic waves and skin tissue at ISM band. However, the material is not suitable for characterization of comprehensive body parts such as constructing a whole body model. Considering the fluidity of the proposed skin mimicking material a new skin mimicking material which possesses a gel like form is proposed in the following section.

2.3 Characterization of Skin Mimicking Gel for Industrial, Scientific, and Medical (ISM) (2.40 GHz – 2.48 GHz) Band

Characterizing gel like materials both electrically and geometrically identical to human tissues is vital to obtain accurate experiment results. A skin mimicking gel for ISM Band (2.40 GHz -2.48 GHz) is proposed in this section.The skin mimicking gel is

characterized by using oil, (NaCl) salt, ultra ivory, distilled water, and Agarose. Table 2.2 shows the percentages of the ingredients used to characterize the proposed skin mimicking gel.

Before determining the proportions of the ingredients the electrical properties of the ingredients were measured. Fig. 2.7 and Fig. 2.8 shows the relative dielectric constant and the conductivity comparisons respectively of the ultra ivory, oil, and de-ionized water. In this study, the term oil is used instead of pure vegetable oil. All experiments are performed with pure vegetable oil. Obviously, oil has the lowest relative dielectric permittivity and conductivity among all ingredients, also comparing with the formerly used Triton X-100 and DGBE. Ultra ivory also has low electrical properties. The low electrical properties of oil enable us to mimic low water content human tissues such as fat and muscle.

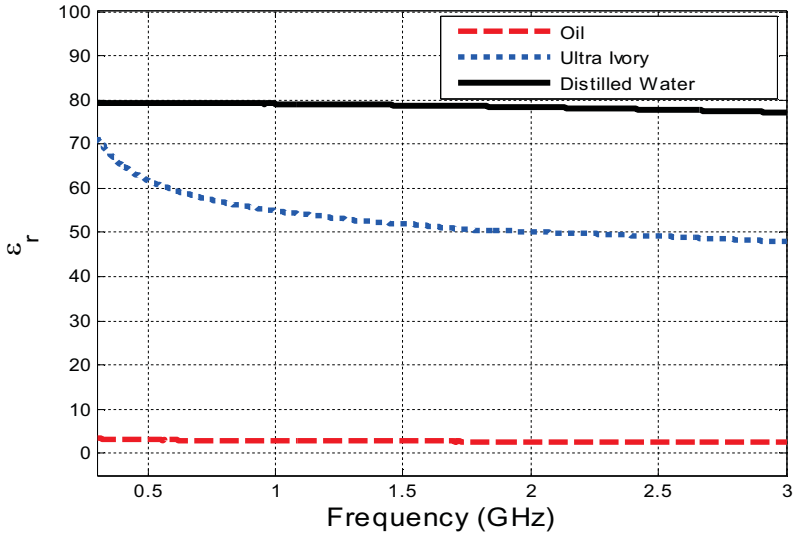

Fig. 2.7 Relative dielectric permittivity comparison of Ultra Ivory, Distilled Water, and Oil.

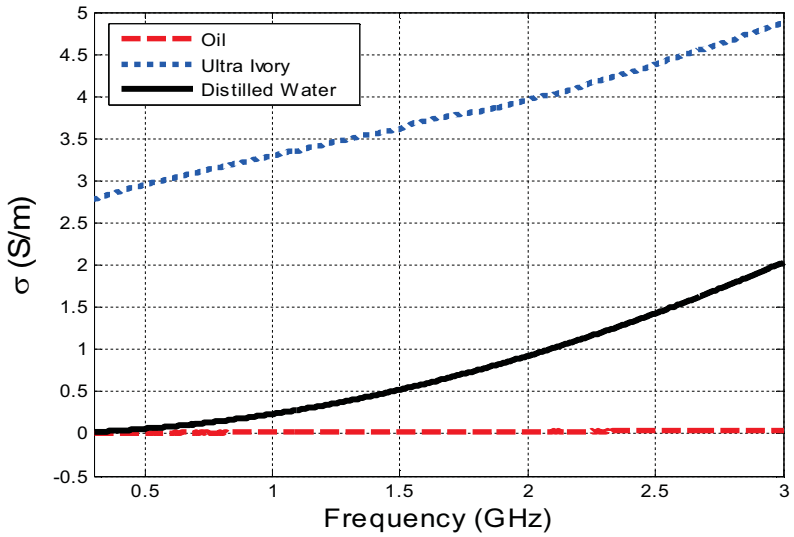

Fig. 2.8 Conductivity comparison of Ultra Ivory, Distilled Water, and Oil.

The experiment steps are important to obtain a uniform gel and highly recommended to be followed when performing the experiment. Water is not a solvent for oil A surfactant is required to solve oil inside the water, ultra ivory has crucial role as a surfactant. To speed up the solving process, also to obtain homogeneous composition of ingredients, oil and distilled water heated until 50 Celsius degree.

Agarose is the ingredient used to solidify the mixture. Agarose is solvable in the water at high temperatures. To compose a well mixed gel like material, agarose added to distilled water, and the mixture is heated until 50 Celsius degree where the mixture become transparent.

The detailed process of mixing ingredients is given step by step in Fig. 2.9. For rapid processing microwave oven is used to heat the ingredients. During the heating of distilled water and oil the bakers covered with microwave safe wraps to prevent vaporization. Salt is added to the mixture to increase the conductivity of the material. The effect of salt to

the electrical properties of the distilled water is investigated by adding 1, 3, 5, and 7 grams of NaCl to 100 ml distilled water. Fig. 2.10 and Fig. 2.11 shows change in the relative dielectric permittivity and conductivity measurements respectively taken by varying the amount of salt in distilled water. Clearly salt is drastically increasing the conductivity of distilled water also decreasing the relative dielectric permittivity of distilled water. The effect of NaCl to the electrical properties is used to increase the conductivity of the skin mimicking gel formulation.

Table 2.2

Recipe for Skin Mimicking Gel

	ISM (2.40GHz – 2.48 GHz)Band
Oil	33%
Deionized Water	66%
Ultra Ivory	1%
Agarose	1.33 grams for 100 ml solution
NaCl	0.4 grams for 100 ml solution

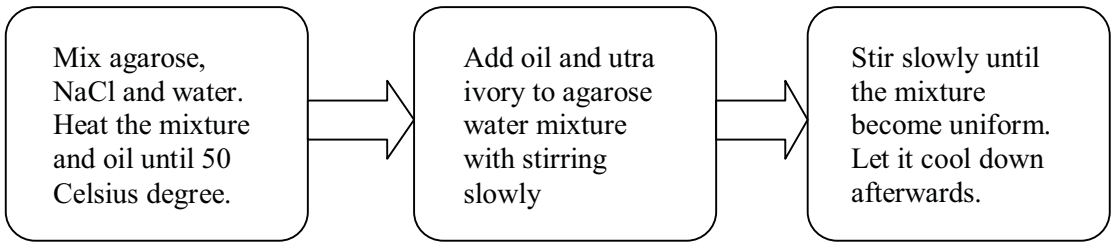

Fig. 2.9. Process for characterizing preparing skin mimicking gel.

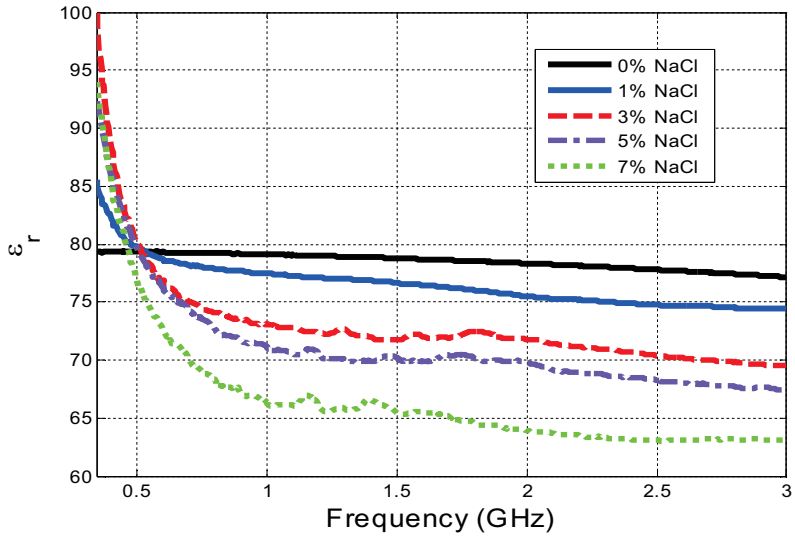

Fig. 2.10 Relative dielectric permittivity comparison of Distilled Water containing various percentages of NaCl.

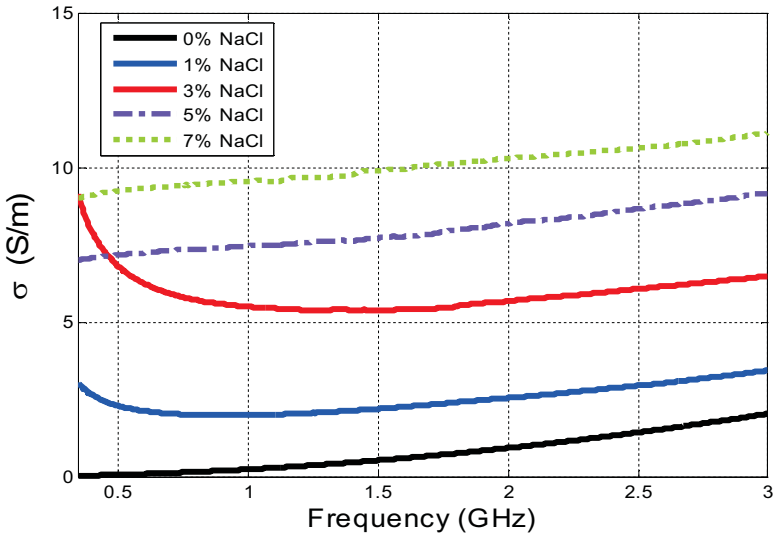

Fig. 2.11 Conductivity comparison of Distilled Water containing various percentages of NaCl.

As stated formerly, agarose is crucial to obtain a gel like material and agarose does not have a significant effect to the electrical properties of the mixture. Considering the

effect of agarose to the electrical properties, we tried to solidify previously formulated mixture prepared by using triton X100, DGBE, and distilled water. However, agarose is not solvable in the mixture proposed in section 2.2. Therefore, using the current recipe is preferable to obtain a gel like skin mimicking material.

The relative dielectric permittivity and conductivity measurements of the proposed skin mimicking gel are given in Fig. 2.12 and Fig. 2.13 respectively. A good agreement obtained both for relative dielectric constant and conductivity between the reference data in [4]-[5] and characterized skin mimicking gel. Since the electrical properties of characterized gel is closely simulates the real human skin between 1.5 GHz to 3 GHz, the skin mimicking gel is suitable for applications requiring wide frequency ranges.

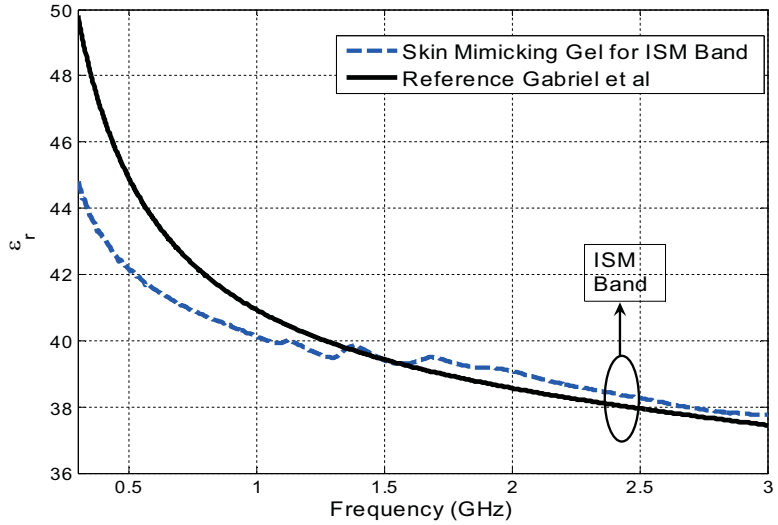

Fig. 2.12 Relative dielectric permittivity comparison of characterized skin mimicking gel and reference data in [4]-[5].

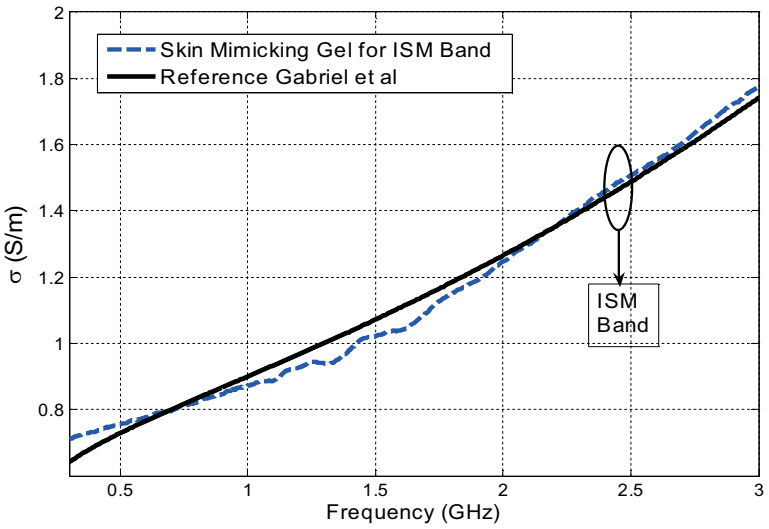

Fig. 2.13 Conductivity comparison of characterized skin mimicking gel and reference data in [4]-[5].

The skin mimicking gel has a solid structure where it can be used to construct a whole body model, without any interaction with other tissue mimicking materials such as muscle, and fat. The potential applications for skin mimicking gel can be, but not limited to, testing of newly developed medical equipments such as tomographic tools, testing of implantable devices, specific absorption rate (SAR) measurements, and dosimetry measurements.

2.4 Characterization of Muscle Mimicking Gel for Wide (0.30 GHz – 2.50 GHz) Band

So far many applications requiring investigation the interaction between biological tissues and electromagnetic waves such as cell phones, artificial eyes, brain and cardiac pacemakers, has been tested with simplified biological tissue models. However, wave

propagation on tissues is effected by thickness, electrical properties, and the physical properties of tissues. Characterizing the tissue layers is important to compose a realistic tissue model for accurate measurements. To meet the biocompatibility requirements, stable gel like structures is very suitable for testing of such devices. Solid tissue mimicking materials are durable and this enables us to characterize different materials and simply just by combining them, create a realistic model of human tissue layers.

In this section, a muscle mimicking gel, simulating the electrical properties of human muscle between 0.30 GHz and 2.50 GHz is proposed.

Table 2.3

Recipe for Muscle Mimicking Gel

	(0.30GHz – 2.50 GHz)Band
Oil	40%
Deionized Water	58%
Ultra Ivory	2%
Agarose	1.33 grams for 100 ml solution
NaCl	0.3 grams for 100 ml solution

The muscle mimicking gel is obtained by varying the percentages of ingredients used to characterize the skin mimicking gel proposed in section 2.3. The recipe for the muscle mimicking gel is given in Table 2.3Since the conductivity and dielectric permittivity of human muscle is lower than human skin, the proportion of oil is increased. The proportion of distilled water and salt is decreased. As the percentage of the oil increases the mixture will have a whitish color. The detailed process to obtain a muscle mimicking gel is identical with the detailed process given in Fig. 2.9. Note that the

process is identical with skin mimicking gel's process except from proportions of ingredients. In Fig. 2.14 characterized tissue mimicking gels are showed.

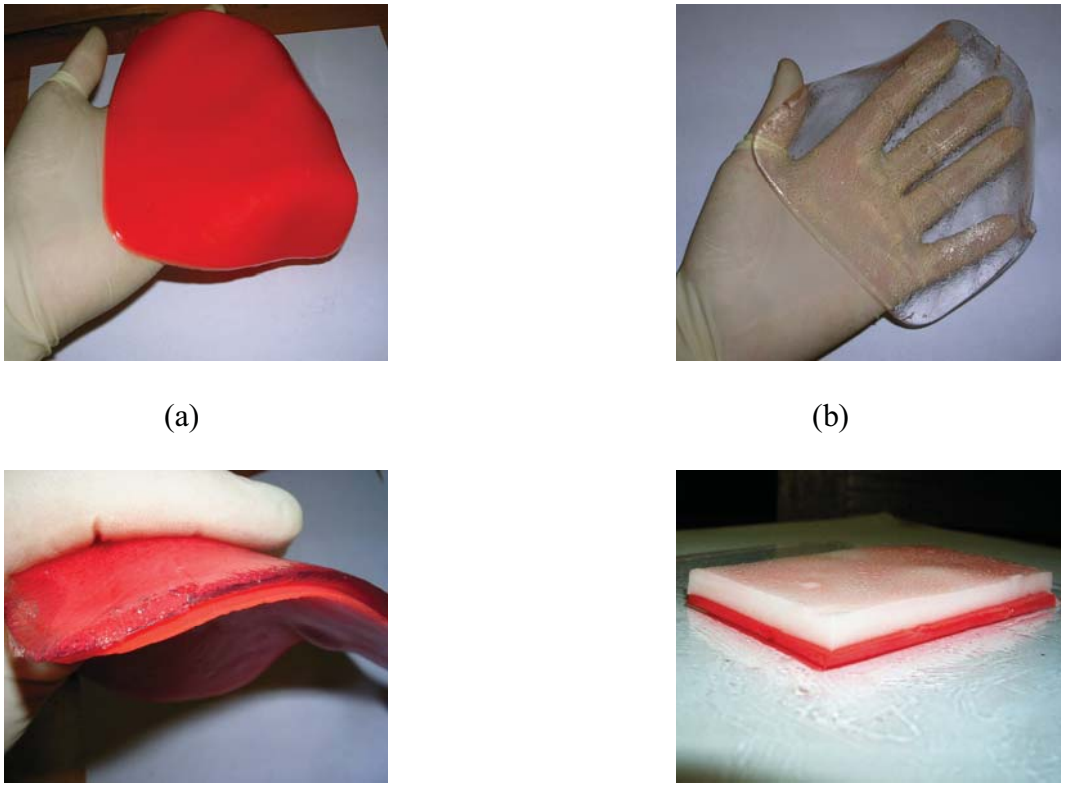

(a) (b)

(c) (d)

Fig. 2.14 (a) Wide band muscle mimicking gel, (b) skin mimicking gel for MICS Band, (c) Two layered tissue mimicking material for MICS Band, (d) Two layered tissue mimicking material for ISM Band.

Fig. 2.15 and Fig. 2.16 shows the dielectric permittivity and conductivity comparisons with the characterized muscle mimicking gel and the reference data respectively. A very good agreement obtained between the tissue simulating material and the reference data in [4]-[5] for wide band from 0.3 GHz to 2.50 GHz.

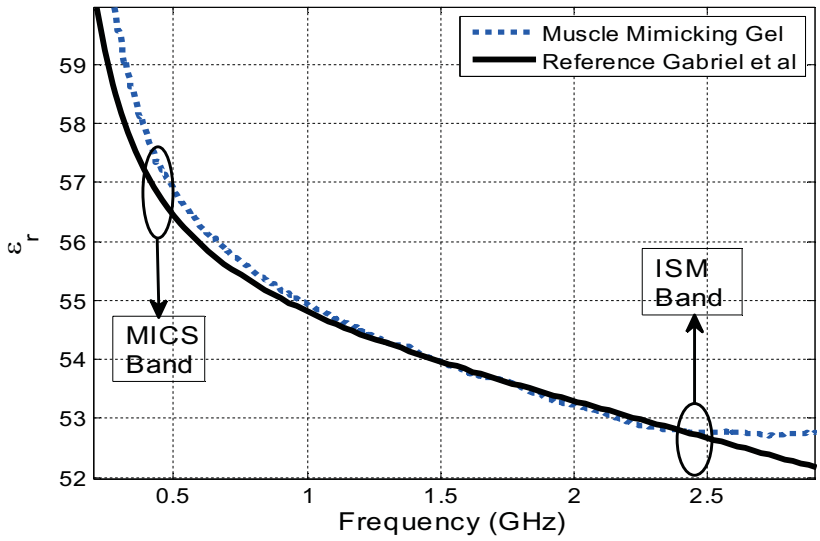

Fig. 2.15 Relative dielectric permittivity comparison of characterized muscle mimicking gel and reference data in [4]-[5].

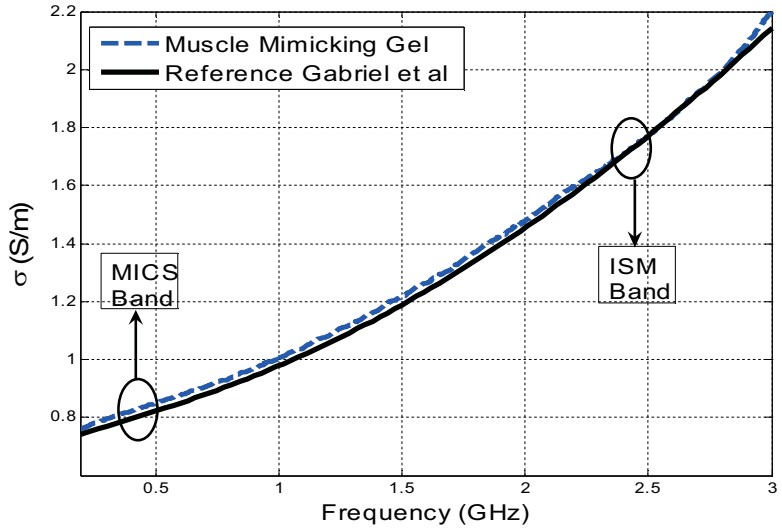

Fig. 2.16 Conductivity comparison of characterized muscle mimicking gel and reference data in [4]-[5].

An error analysis performed for 0.30 GHz and 2.50 GHz band. As seen, the maximum error in the 0.3 GHz – 2.50 GHz band is

$$Error_{\varepsilon_r} = \frac{|\varepsilon_{r(material)} - \varepsilon_{r(human)}|}{\varepsilon_{r(human)}} < 2.23\% \tag{3}$$

for relative dielectric constant and

$$Error_{\sigma} = \frac{|\sigma_{material} - \sigma_{human}|}{\sigma_{human}} < 6.7\% \tag{4}$$

for conductivity.

CHAPTER III

IN VITRO TESTING OF IMPLANTABLE ANTENNAS AND MUTUAL COUPLING MEASUREMENTS OF ON BODY ANTENNAS

3.1 Overview

Recently, there is a growing research activity on wireless telemedicine application for monitoring various physiological parameters of human body such as, nerve signal recorders, implantable myoelectric sensors, and telemetry monitoring systems [8]-[10]. The antennas are key components for monitoring systems, since they should effectively transmit data between the implantable or on body device and the exterior unit. The design of such an antenna is a quite challenging task due to the compatibility issues with both lossy tissue media and the implantable or on-body sensor system. In addition, the antenna should meet the small size, low cost, high efficiency, large bandwidth, and low power requirements.

Microstrip antennas are widely used for telemetry systems due to their benefits such as, low cost, ease of fabrication, light weight, and compatibility with the other circuitry [11]-[13]. Although the microstrip antennas meet some critical requirements of telemetry systems, the operational disadvantages such as narrow frequency bandwidth, low power, and low efficiency are not desirable for monitoring application.

Several techniques can be used to eliminate disadvantages of microstrip antennas such as, increasing the electrical length of the antenna, using thick substrate, and using a superstrate that helps to increase the bandwidth [14]-[16]. The optimal conditions of a microstrip antenna can be designed either by trial and error method or by employing the heuristic optimization algorithms. Since the trial and error method may require many trials which is time consuming and does not guarantee to reach the optimal design, it is not an effective technique for antenna design. On the other hand, heuristic algorithms such as particle swarm optimization (PSO) and genetic algorithms (GA) are far more effective and widely used in the design of microstrip antennas [17]-[19].

In this chapter, design and *in vitro* testing of an implantable serpentine shaped dual band antenna and mutual coupling measurements for a wireless cardiac monitoring system are presented. The design and fabrication of the implantable antenna is explained in section 3.2. Section 3.3 discusses the testing of the implantable antenna with skin mimicking material proposed in section 2.2 and with two layered tissue mimicking material (skin and muscle) proposed in section 2.3 and 2.4. Section 3.4 explains the design of an on-body antenna, and finally, section 3.5 discusses the mutual coupling measurements of on-body antennas.

3.2 Design and Fabrication of a Serpentine Shaped Implantable Antenna

A serpentine shape is considered for the design of the antenna to obtain large electrical length. A shorting pin is also used to enable further antenna miniaturization. Rogers RO3210 material with $\varepsilon_r = 10.2$ dielectric constant is used for both substrate and

superstrate. Using a substrate with high dielectric constant allows a higher bandwidth. After the initial design, the dimensions of the antenna are optimized by using hybrid PSO-HFSS technique. Initial design for the antenna is given in Fig. 3.1a.

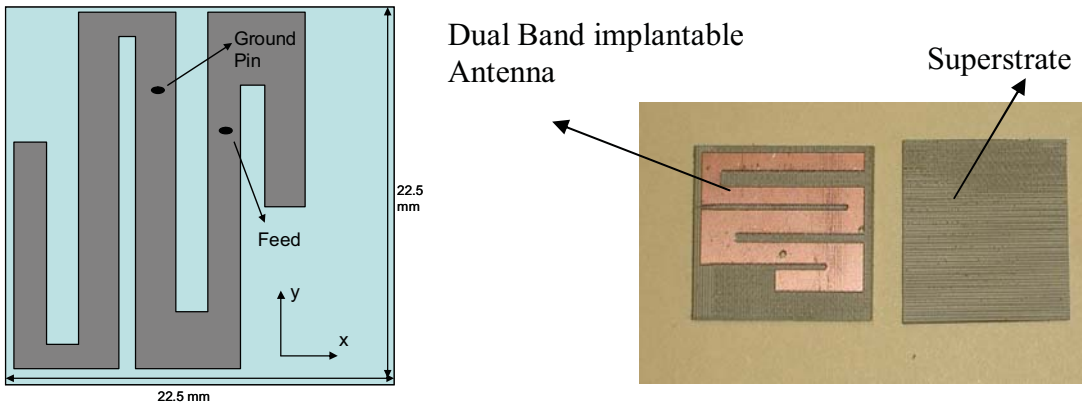

(a) (b)

Fig. 3.1 (a) The top view of initial design for antenna, (b) top view of fabricated antenna.

PSO algorithm is developed by Kenedy and Eberhart in 1995 [20]. PSO is used in many diverse application areas one of which is in antenna optimization. As an analogy, behavior of a bee swarm can be used to present the conceptual overview of the algorithm. The bees start searching a field in random places without a prior knowledge. Each bee records the location of the field with the most flower density where it encountered. Then, somehow it knows the locations with abundance of flowers found by other bees in the swarm. The uncertain bee changes its direction by flying between the location found by itself with the highest density of flowers and the location found by other bees in the swarm reported with the highest density of flowers. Once in a while, bee flies over a location with the highest density of flowers in the field, then whole bees swarm around

between that location and their own discovery. By over flying on the locations with the highest density the bees explore the field. Unable to find locations with higher density of flowers the swarm is drawn around the field with the highest density of flowers. Specific terms used in PSO language are given in Table 3.1 [21]. For an antenna optimization problem, the position can be the amplitude and phase of element excitation in a phased array, and the fitness can be the antenna gain, peak cross-polarization, and return loss of the antenna. An implementation script between MATLAB computing language and High Frequency Structure Simulator (HFSS) electromagnetic simulation program as well as a simple, flexible PSO algorithm developed in MATLAB computing language is used for the optimization of the implantable antenna [22]-[23]. The flowchart of the PSO algorithm used for optimization of the implantable antenna is given in Fig. 3.2. Details regarding the antenna optimization are given in [23].

Table 3.1

Specific Terms Used in PSO Language

Particle	One single individual in the swarm
Location	An Agent's N dimensional coordinates which represents a solution to the problem
Swarm	The entire collection of particles
Fitness	A single Number Representing the goodness of a given solution
Pbest	The location in parameter space of the best fitness returned for a specific particle (personal best)
Gbest/Pg	The location in parameter space of the best fitness returned for the entire swarm (global best)
Velocity	The velocity of the particle that is decided according to pbest and gbest.

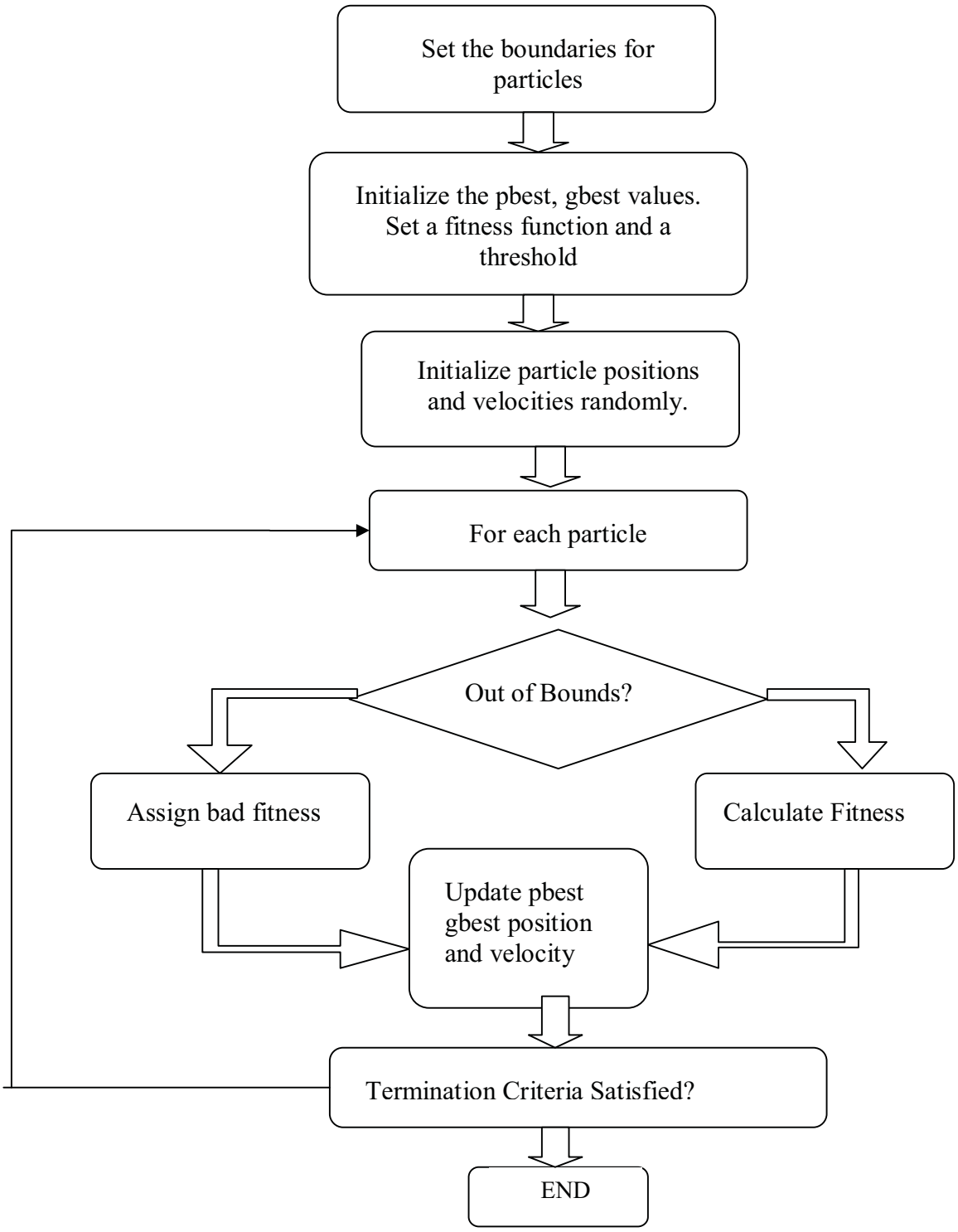

Fig. 3.2 Flowchart of the algorithm for antenna optimization in [22].

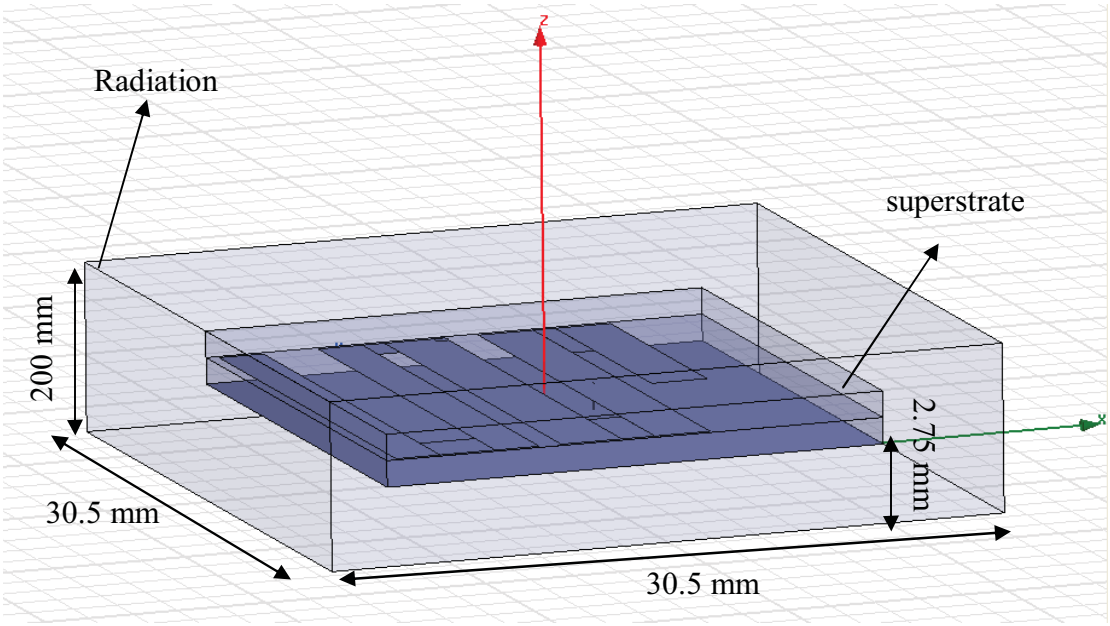

(a)

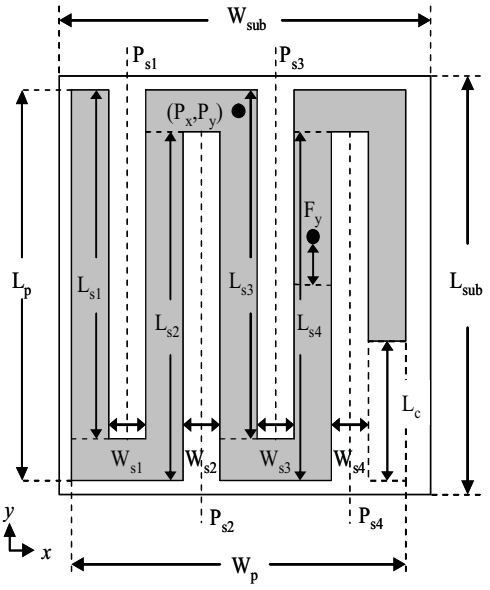

(b)

Fitness Function

$$fitness = \max\left(S_{11@402\,\mathrm{MHz}}, S_{11@2.4\,\mathrm{GHz}}\right)$$

Constraints

$$L_{si} < L_p, i = 1,2,3,4 \qquad P_{s1} - \frac{W_{s1}}{2} > -10.75$$

$$P_{s4} + \frac{W_{s4}}{2} < -10.75 + W_p \qquad L_c < L_{s4}$$

$$P_{si} + \frac{W_{si}}{2} < P_{s(i+1)} - \frac{W_{s(i+1)}}{2}, i = 1,2,3$$

(c)

Fig. 3.3 (a) The computational model of implantable antenna, (b) the optimized parameters of antenna, (c) fitness function and constraints used to optimize the antenna.

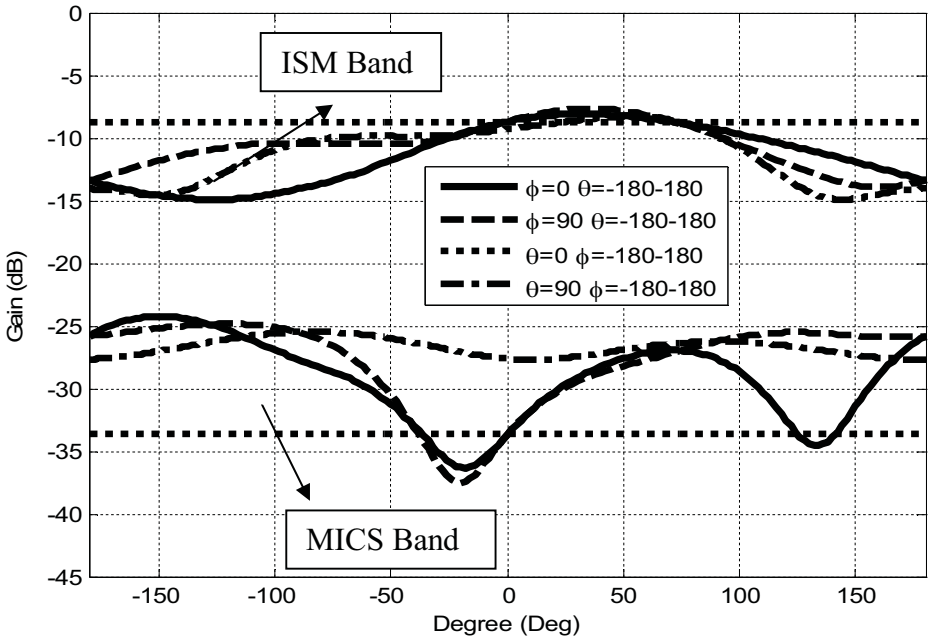

(a)

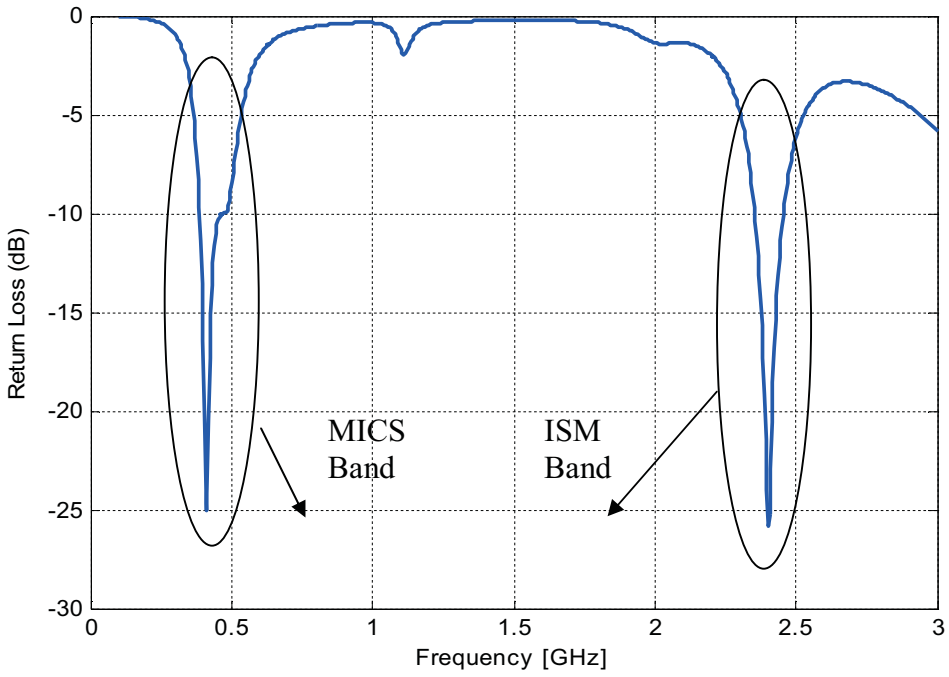

(b)

Fig. 3.4 (a) Simulated gain pattern, (b) Simulated return loss of the antenna.

The HFSS model of the antenna is given in fig 3.3 a. The optimized parameters in PSO are given in Fig 3.3 b. The gain pattern and the return loss of the optimized dual band implantable antenna is given in Fig. 3.4 a and Fig. 3.4 b respectively [23]. The significance of ISM band is to enable the power conservation with a wake up signal. This provides longer lifetime to the implant. The MICS band is for gathering and transferring the required data. The optimized values of antenna parameters are given in table 3.2.

Table 3.2

The optimized values of the antenna parameters

Symbol	Range (mm)	Optimized (mm)
P_{s1}	[-8 , -6]	-7.0
W_{s1}	[0.5 , 3]	2.7
L_{s1}	[19 , 21]	19.1
P_{s2}	[-4 , -3]	-3.9
W_{s2}	[0.3 , 3]	0.5
L_{s2}	[19 , 21]	20.1
P_{s3}	[0 , 1]	0.5
W_{s3}	[0.5 , 3]	2.0
L_{s3}	[17 , 18.5]	18.0
P_{s4}	[3.0 , 4.5]	3.5
W_{s4}	[0.5 , 3]	0.6
L_{s4}	[16.5 , 18.5]	17.5
L_c	[6 , 11]	9.6
F_y	[- 2, 2]	0.1
P_x	[0.1 , 1.5]	0.2
P_y	[0.1 , 5]	0.2

3.3 *In vitro* Testing of an Implantable Antenna

The skin mimicking material for ISM band proposed in section 2.2 is used for *in vitro* testing of the implantable antenna designed in [23]. First, the antenna is placed on the base of a plastic container with dimensions 12 cm x 8.5 cm x 3 cm, and then the skin mimicking material with a depth of 1 cm is poured into the container. The measurement set up is shown in Fig. 3.5. The thickness of the skin mimicking material is 4 mm both from the top and bottom of the antenna as it approximates the thickness of the real skin tissue. The return loss measurement is performed using E8362B PNA network analyzer.

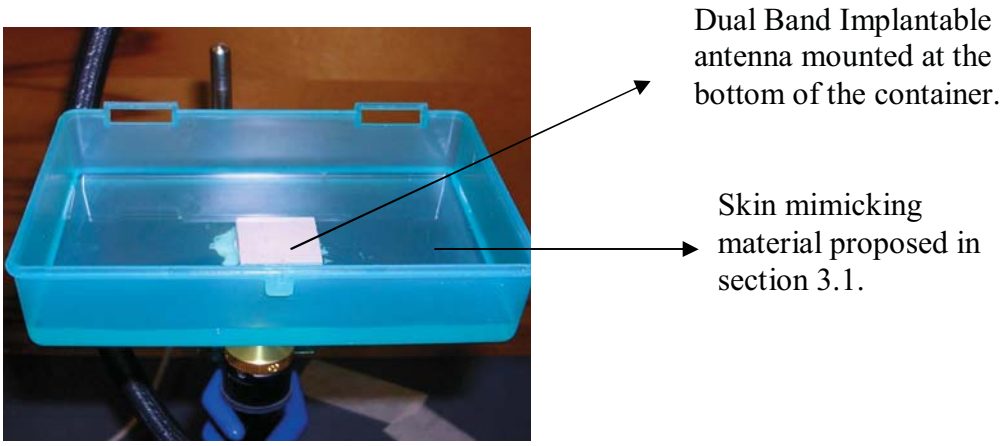

Fig. 3.5 Measurement set-up for *in vitro* testing of the implantable antenna with skin mimicking material for ISM band.

Fig. 3.6 shows a comparison for the measured and simulated return loss. The simulation is performed using our in-house finite element boundary integral solver (FE-BI). Note that skin mimicking material simulates the electrical properties of human skin for ISM band; and therefore, a good agreement for return loss is expected and achieved

for ISM band measurement. The measured return loss for ISM band is -20 dB which shows a good agreement with the simulation.

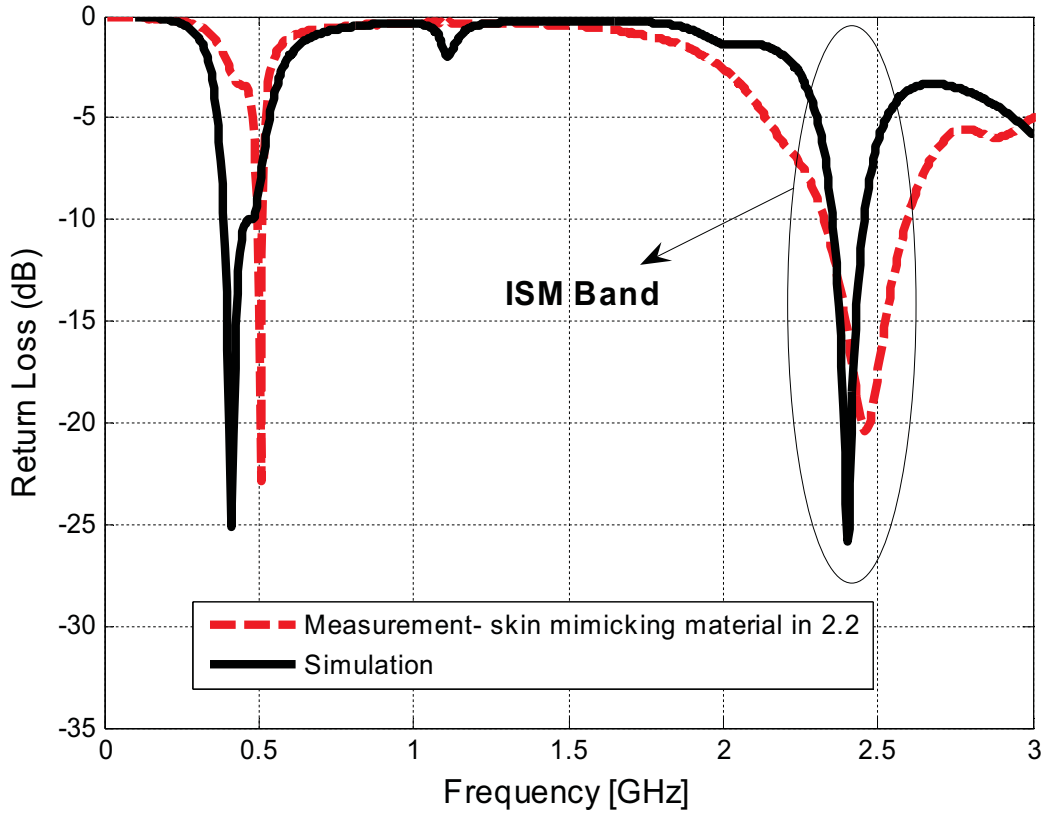

Fig. 3.6 Return loss measurement results of the implantable antenna with ISM band skin mimicking material in 2.2.

In order to investigate the effect of the tissue layers beneath the antenna, the antenna is also tested *in vitro* with double layered (muscle, skin) tissue mimicking gel for MICS band. The muscle mimicking material proposed in section 2.4 is used and the skin mimicking material is characterized in [23] by mixing sugar, NaCl, distilled water, and agarose. The recipe for the skin mimicking gel is given in Table 3.3 [23]. First, the 2.1 mm muscle mimicking gel is placed to the bottom of the container with dimensions 12

cm x 8.5 cm x 3 cm. The antenna is mounted above the muscle mimicking gel by placing a hole for the connector (see Fig. 3.7a). After that, skin mimicking gel for MICS band is placed above the antenna and muscle mimicking material (see Fig. 3.7 b). The measurement set-up is given in Fig. 3.7 c. The return loss measurement is given in Fig. 3.8.

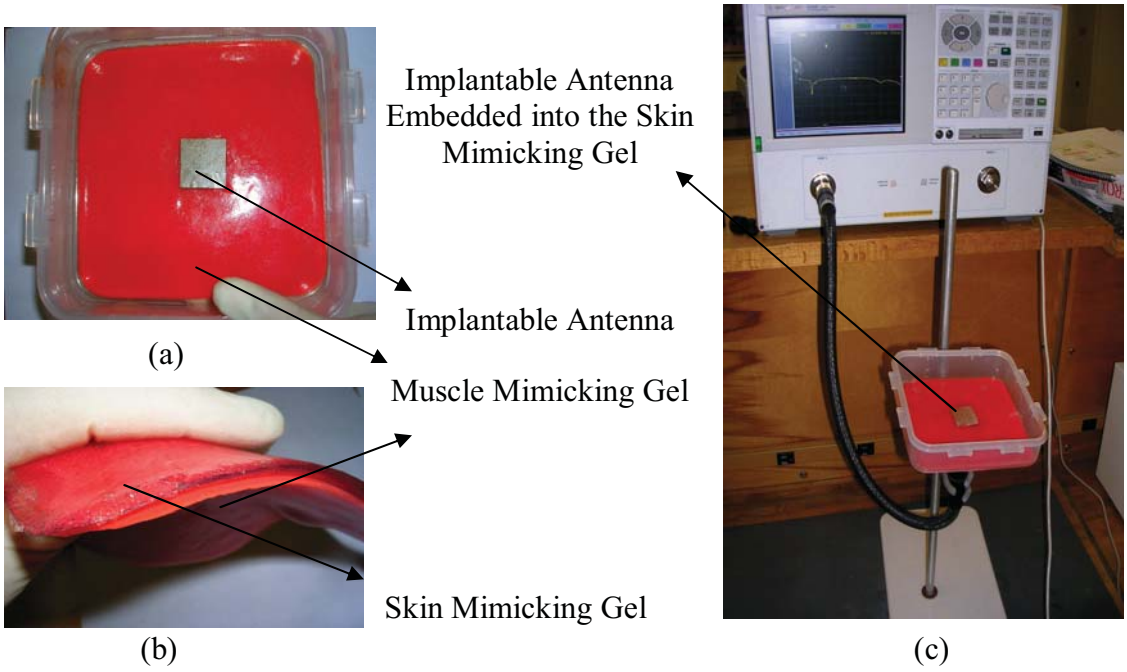

Fig. 3.7 (a) Implantable antenna mounted at the bottom of a container, (b) wide band muscle mimicking gel and MICS band skin mimicking gel, (c) the measurement set up.

Measured return loss agreed well with the simulation results for the MICS band. From the experiment, it is seen that the muscle layer lying below the antenna does not have a significant effect on the antenna performance.

Table 3.3

Recipe of Skin Mimicking Gel for MICS Band in [23]

Sugar	56.18%
NaCl	2.33%
Distilled Water	41.49%
Agarose	Add 1 gram in 100ml solution

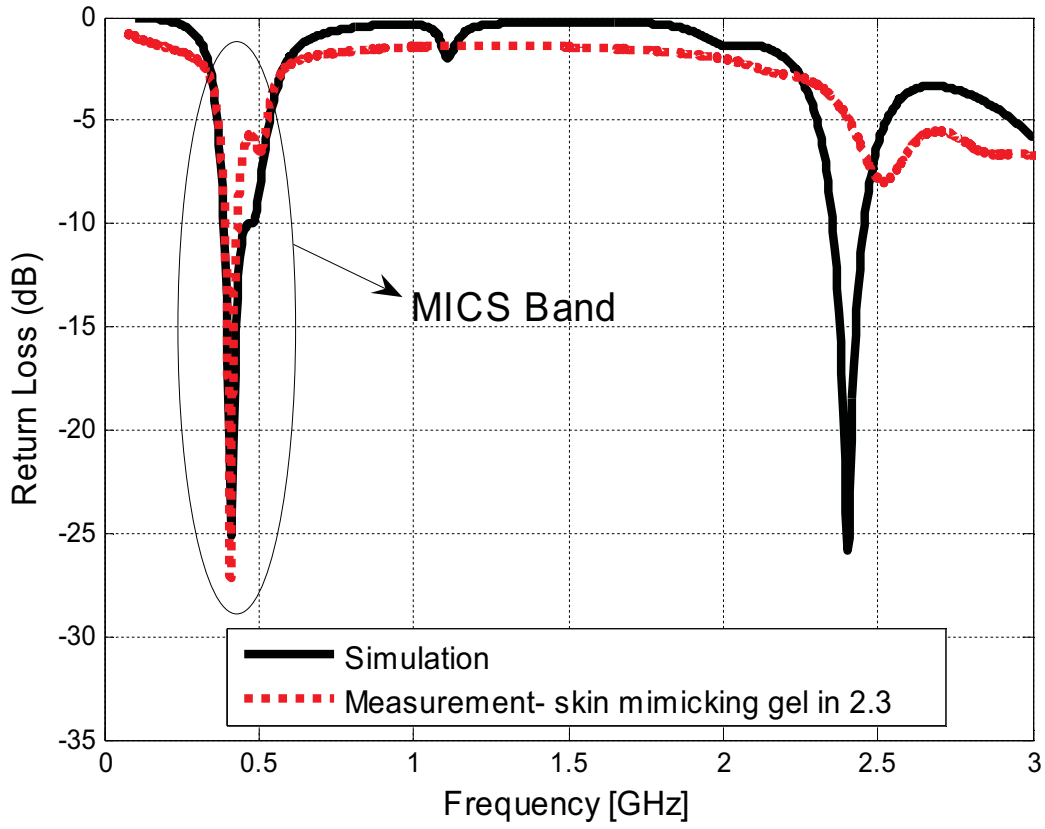

Fig. 3.8 Return loss measurement results with double layered (muscle and skin) tissue mimicking materials.

3.4 Design of On-body Antenna

Electrocardiogram (ECG) monitoring is important to diagnose heart abnormalities and treat patients with cardiac related diseases. ECG monitoring systems normally employ at least three electrodes where the electrodes are collecting data and wired back to a central monitoring system for data transmission. In a traditional monitoring system the wires can be tangled up that causes the electrodes to be dislodged from patients body. To improve patient's comfort, developing a wireless cardiac monitoring system is vital. Cardiac care based on an out-patient setup through the wireless cellular or internet network is the key to improve the current cardiac monitoring systems. Monitoring the cardiac data of the patient from the cardiologist office and designing a system with wireless electrodes not only provide better conditions for patients but also reduce the medical costs. Designing body-centric antennas is a key component to develop such systems [24]-[26]. These antennas are intended to provide the communication between the sensors and an external data storage unit. However, there are several challenges in the design of such antennas. The antennas have to be small enough to be mounted on the body and have sufficient gain to transmit data to the required distance [27]-[29]. In addition, the mutual coupling between the antennas should be minimized to ensure a reliable data transmission.

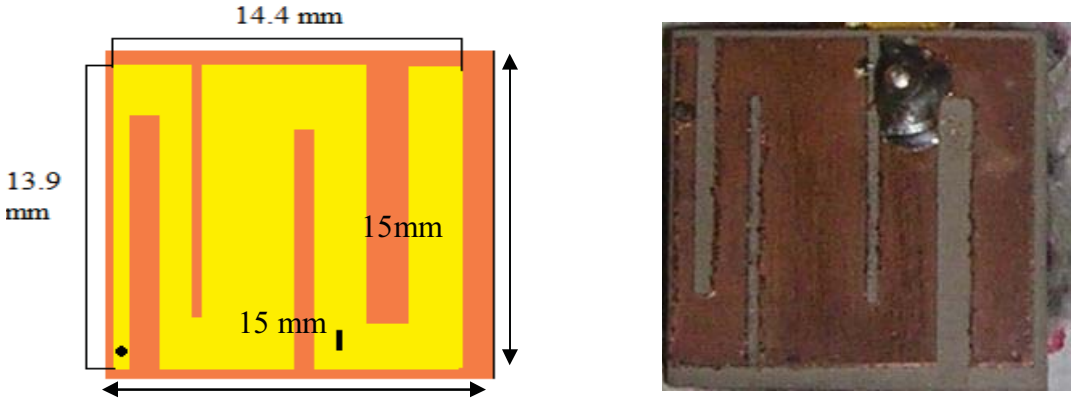

Fig. 3.9 Dimensions of the on-body antenna and the fabricated on-body antenna.

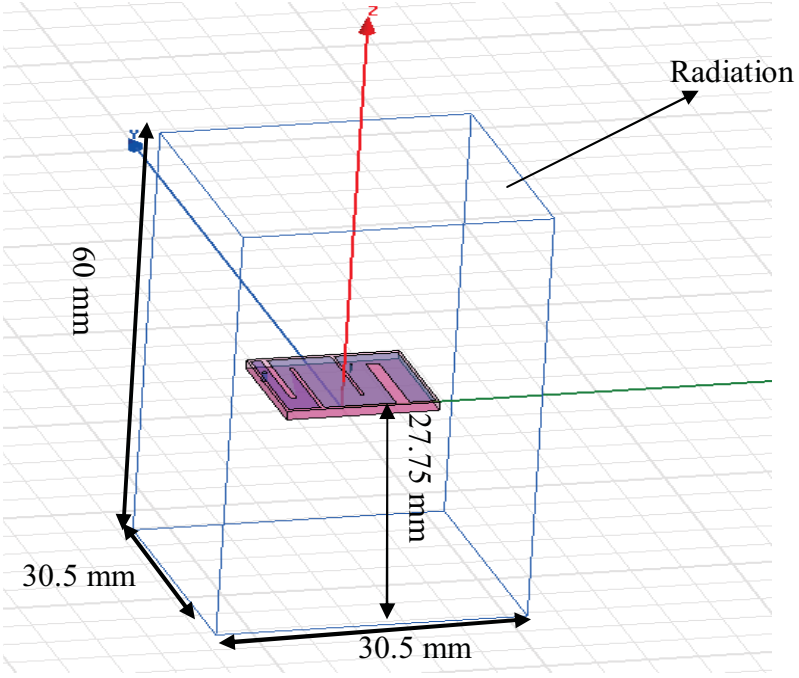

Fig. 3.10 The computational model of implantable antenna.

Comparison between the return loss simulation and measurement of the antenna is given in Fig. 3.11. As seen, Fig. 3.11 the measurement and the simulation results agree well.

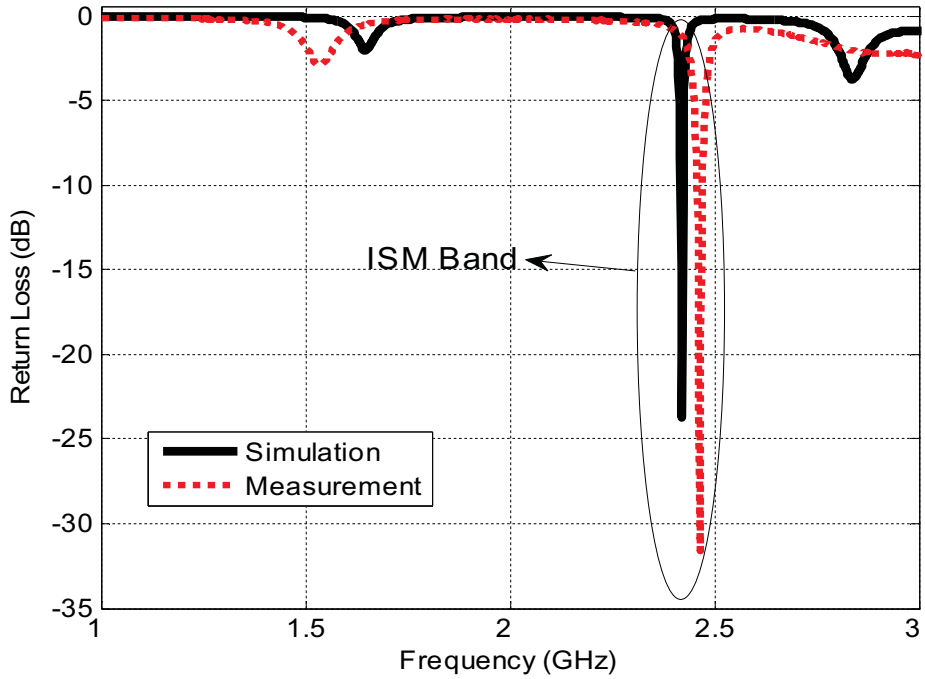

Fig. 3.11 Comparison between return loss simulation and measurement of the antenna.

In this section, the design of a small size microstrip antenna operating at ISM band is described. The antenna is designed to be integrated into the wireless ECG system to provide communication between the electrodes and the central monitoring unit. To do so, the initial design of the antenna is composed by using trial and error method, and then the dimensions of the antenna are optimized by employing the PSO algorithm described in section 3.1 in combination with finite HFSS. The antenna is printed on Rogers RO3210(tm) substrate and the return loss measurements are performed with E8362B

network analyzer in air. The dimensions of the antenna are given in Fig. 3.9, and the computational model of ISM band on body antenna is given in Fig. 3.10. Note that the computational model is designed by using HFSS software.

3.5 Mutual Coupling Measurements

In this section, mutual coupling between on-body antennas has been investigated experimentally by series of measurements of the S-parameters. The coupling effects between on body antennas may produce increased side lobe level, main beam squint, filled or shifted nulls, and grating lobes. Therefore, it would be of substantial value to be able to predict coupling effects on the system performance.

To perform mutual coupling measurements, two identical on-body antennas proposed in section 3.4 are fabricated. In order to investigate the effects of tissue layers beneath the antennas, three different measurement configurations are formed. First set of measurements are performed by mounting the antennas on a cardboard. Then, the antennas are mounted on a cardboard covered with a single layer skin mimicking material, and then on a cardboard covered with three layered (skin, muscle, and fat) tissue mimicking material. Rectangular three layered tissue mimicking material is used to approximate a children torso. Three layered tissue mimicking gel is composed of skin mimicking gel for ISM band proposed in section 2.3, wide band muscle mimicking gel proposed in section 2.4, and the fat mimicking gel in [30].

Table 3.4

Recipe of Fat Mimicking Gel [30]

gelatin type A	34 grams Dry Mass
2 propanol	10 ml
p-toulic acid (powder)	0.2 grams
distilled water	190 ml
oil (pure vegetable)	800ml
ultra ivory	11.2ml
formaldehyde	2.16 grams

The recipe for fat mimicking gel is given in Table 3.4. For single layered media the skin mimicking gel proposed in section 2.3 is used. Antennas are mounted on surfaces with the main radiating elements facing outward. The measurement set up is illustrated in Fig. 3.12. All measurements are performed with Agilent's E8361B network analyzer. The antennas are placed in 8 different configurations and measurements are taken accordingly. The configuration of three layered tissue mimicking material is given in Fig. 3.13.

According to S_{12} measurements, the mutual coupling level decreases monotonically with increasing separation between the antennas. The antennas are placed with various distances and mutual coupling measurements are taken. According to the measurement results, it has been seen that if the antennas are placed more than 40 millimeters of distance, the mutual coupling is ignorable. Therefore, tests are performed for 40 mm, 30 mm, and 20 mm separations.

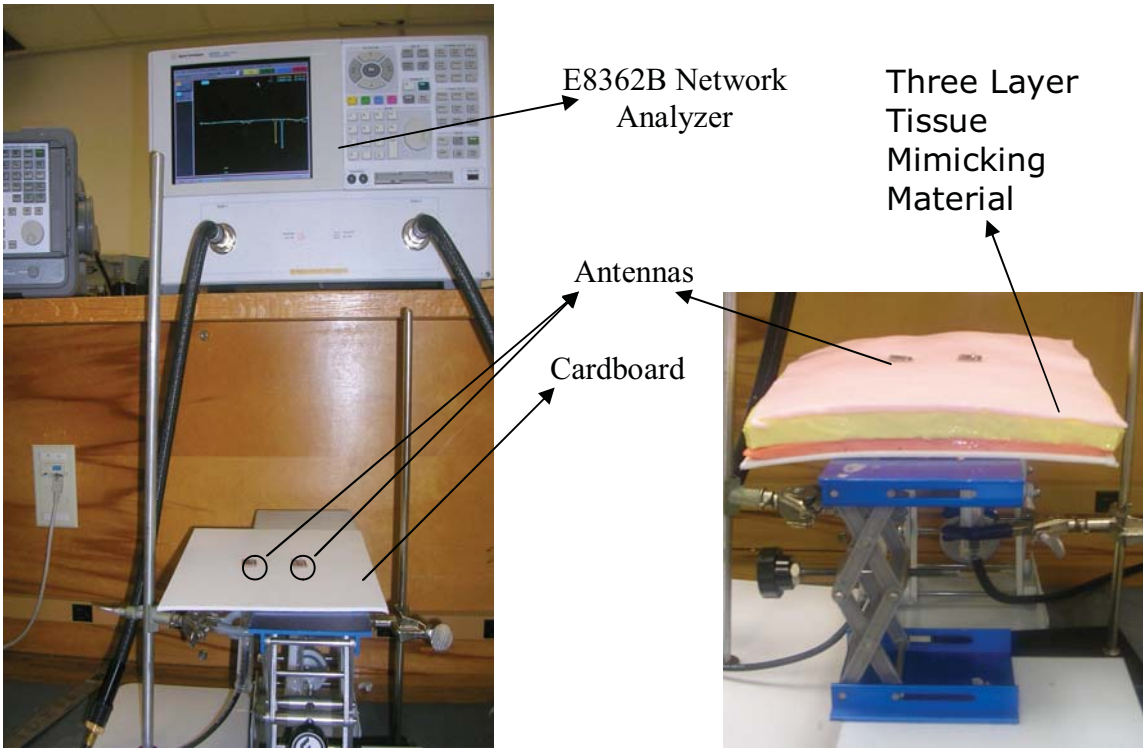

Fig. 3.12 (a) Two identical on-body antennas operating at ISM Band mounted on a cardboard, (b) antennas mounted on a three layered tissue mimicking material.

The close distance measurements are performed considering the applications of the cardiac monitoring system for children patients. Eight different combinations are formed by placing antennas with different angles and total of 127 measurements were taken. From the measurement results, it has been concluded that mutual coupling can be minimized by placing the antennas with 90 degree difference between them. The measurement results are given for symmetrically placed antennas (0 degree difference) and for the alignment with minimum mutual coupling (90 degree difference).

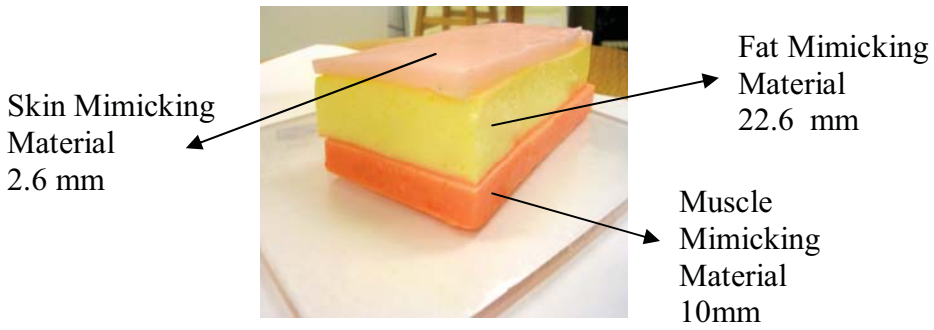

Fig.3.13 Three layered tissue mimicking material composed of skin, fat and muscle layers.

The computational model of the mutual coupling measurements is given in Fig. 3.14. The computational model is designed in HFSS software program and S_{12} mutual coupling simulations are taken accordingly. The given model shows two symmetrically positioned on-body ISM band antennas placed with 20 mm distance on air media.

The measurements are performed for fixed distance by changing the tissue layer beneath the antenna. Fig. 3.15a shows the comparison of fixed distance 40 mm between two on-body antennas for different layers beneath the antenna. . Mutual coupling measurements for skin and three layered tissue mimicking material show close proximity to each other.

As observed from the results, the measurements taken at 2.4 GHz are significantly different for the air media. The difference is between 15 dB to 20 dB which indicates that the tissue layers have a significant effect on mutual coupling between two antennas. Fig. 3.15b shows the comparison between measurements and simulation for mutual coupling on single layered media.

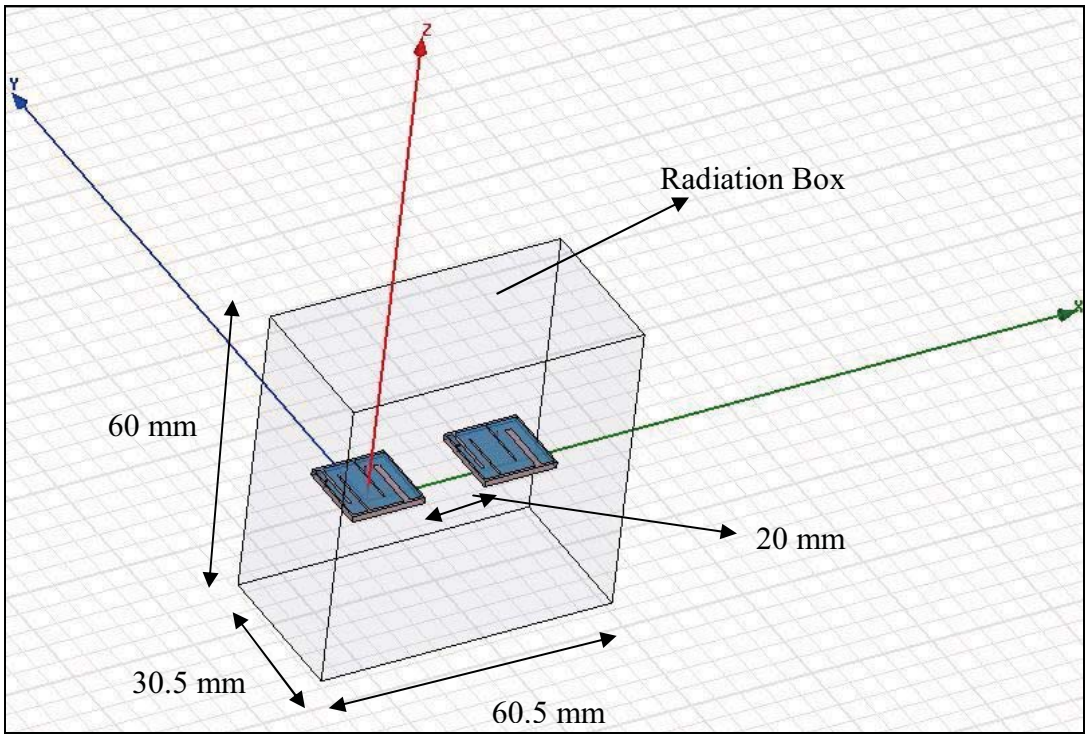

Fig. 3.14. Computational model of mutual coupling between two identical ISM band on-body antennas

The simulation and measurements comparison for air also is shown in Fig. 3.15b and Fig. 3.15c. For both Fig. 3.15b and Fig. 3.15c the trend of mutual coupling simulation is similar with the trend of mutual coupling measurements. The comparisons show the accuracy of the measurements.

Fig. 3.16 illustrates the experiment set-up for symmetrically placed antennas mounted on human torso approximation with a 30 mm distance. The measurements for 30 mm are performed on air media, single (skin mimicking) layered media, and three layered media.

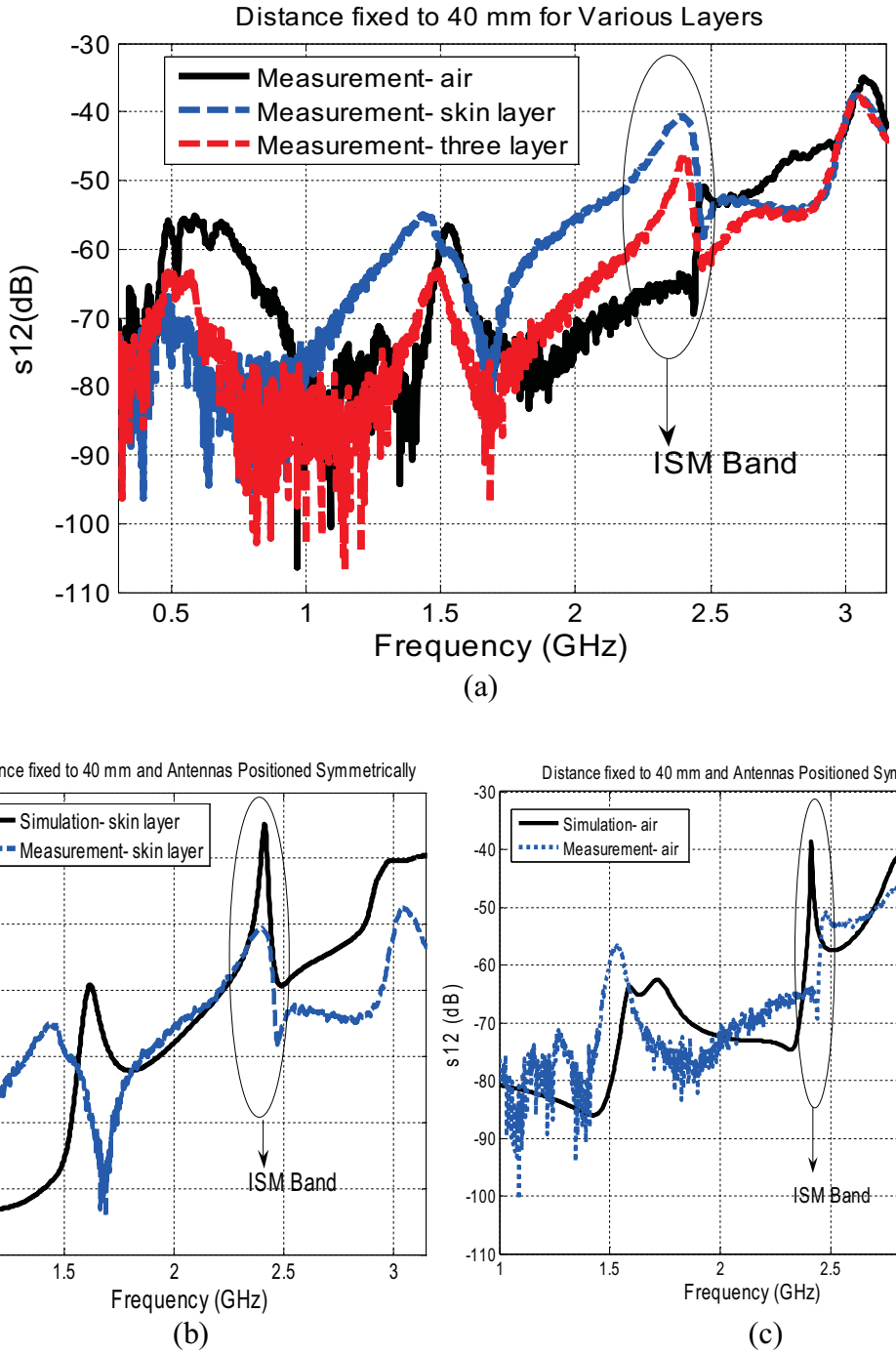

Fig 3.15 (a) Mutual coupling between the antennas for air, single layered, and three layered media (b) Comparison between the simulation and measurement of the single layered media (c) Simulation and measurement comparison for air media.

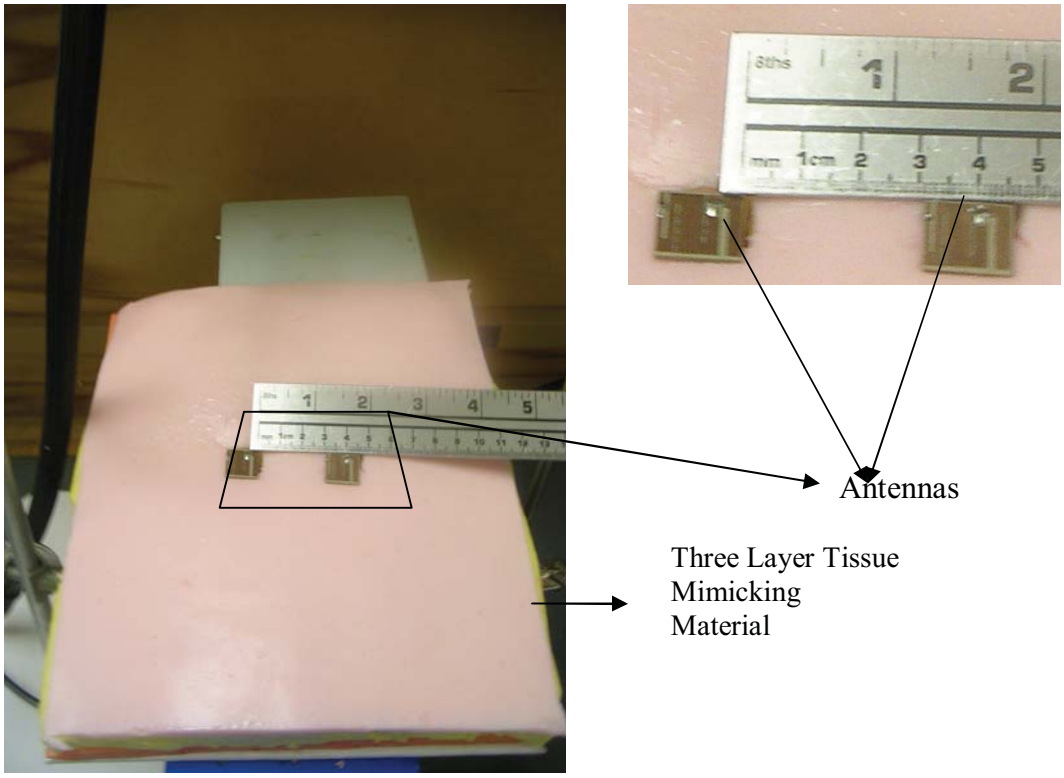

Fig. 3.16 Measurement set up of symmetrically placed antennas mounted on three layered tissue mimicking gel with 30mm fixed distance.

The measurement results regarding the mutual coupling between two identical on-body antennas for the various media is given in Fig. 3.17. Clearly, the mutual coupling is affected by the tissue layers beneath the antenna. The accuracy of the mutual coupling measurements is increased by covering the cardboard with three layered tissue mimicking material. The mutual coupling difference between the air and three layered cases at 2.4 GHz is approximately 20 dB.

A set of measurements are also performed by fixing the distance to 20 mm. The antennas are placed on cardboard (air), skin mimicking gel, and three layered tissue mimicking gel, and the results are given in Fig. 3.18.

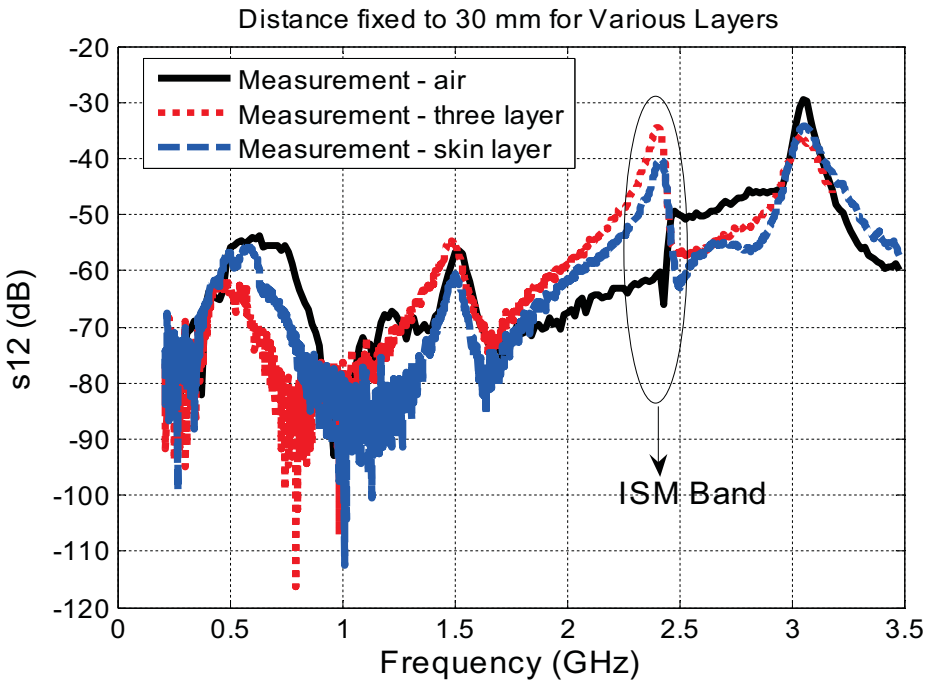

Fig. 3.17 Mutual coupling between the antennas for air, single layered, and three layered media for 30 mm fixed distance.

The calculated measurements prove the necessity of a human torso approximation to investigate the mutual coupling between on-body antennas. Presence of tissue mimicking material beneath the antenna has a significant effect on mutual coupling. There are other factors that affect the mutual coupling between the antennas. One of the significant factors that affect S_{12} directly is the distance between the antennas. In order to investigate the effect of distance, several measurements are taken by varying the distance. As stated formerly, mutual coupling between the antennas becomes significant if the antennas are placed with 40 mm or less distance between one another. Therefore, the measurements are taken for 40 mm, 30 mm, and 20 mm distances between the antennas by changing the surface where the antennas are mounted.

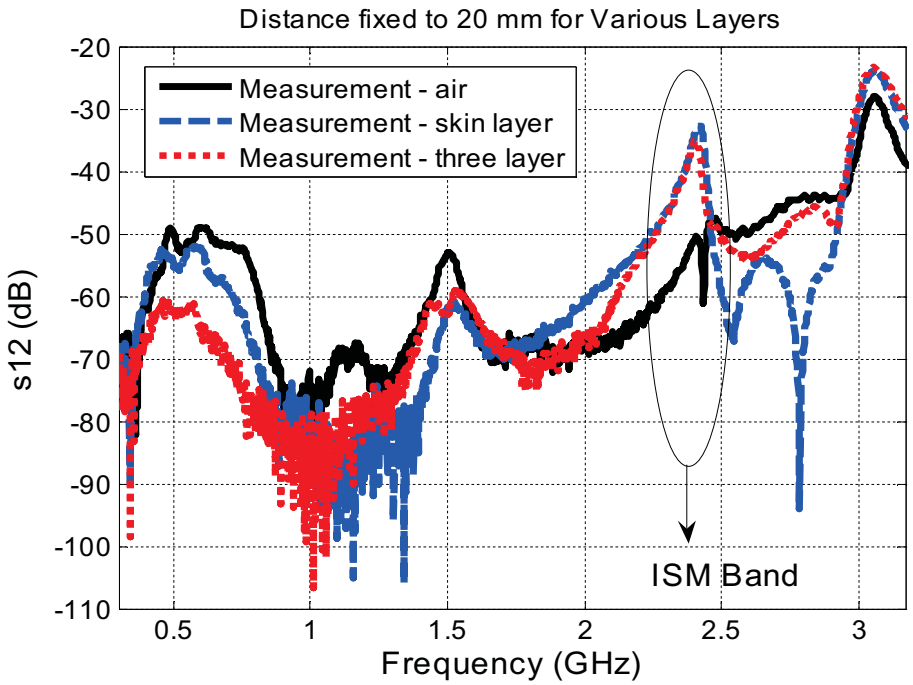

Fig. 3.18 Mutual coupling between the antennas for air, single layered, and three layered media for 20 mm fixed distance.

The first sets of measurements are taken on a cardboard which referred as air media. Measurement results are given in Fig. 3.19. Fig. 3.20 shows the measurements taken by varying the distance between two identical on-body antennas mounted on a skin mimicking material covered cardboard. Finally, Fig. 3.21 shows the mutual coupling measurements for different distances between on-body antennas mounted on three layered tissue mimicking material covered cardboard. The measurements clearly demonstrate that as the distance between the antennas increase the mutual coupling decreases. Note that the antennas are symmetrically positioned during the measurements.

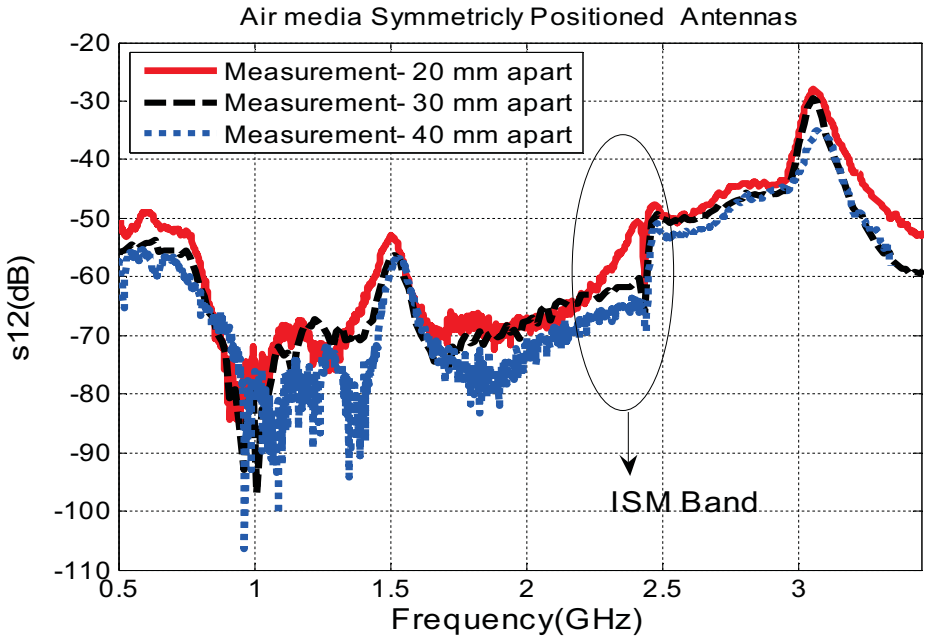

Fig. 3.19 Mutual coupling measurements for antennas mounted 20 mm, 30 mm, and 40 mm apart on a cardboard.

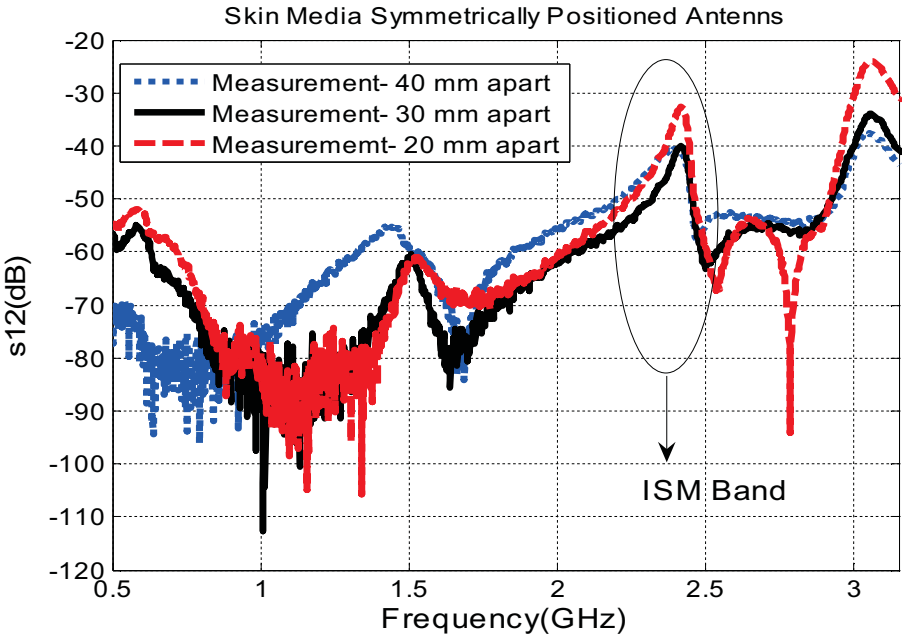

Fig. 3.20 Mutual coupling measurements for antennas mounted 20 mm, 30 mm, and 40 mm apart on skin mimicking gel covered cardboard.

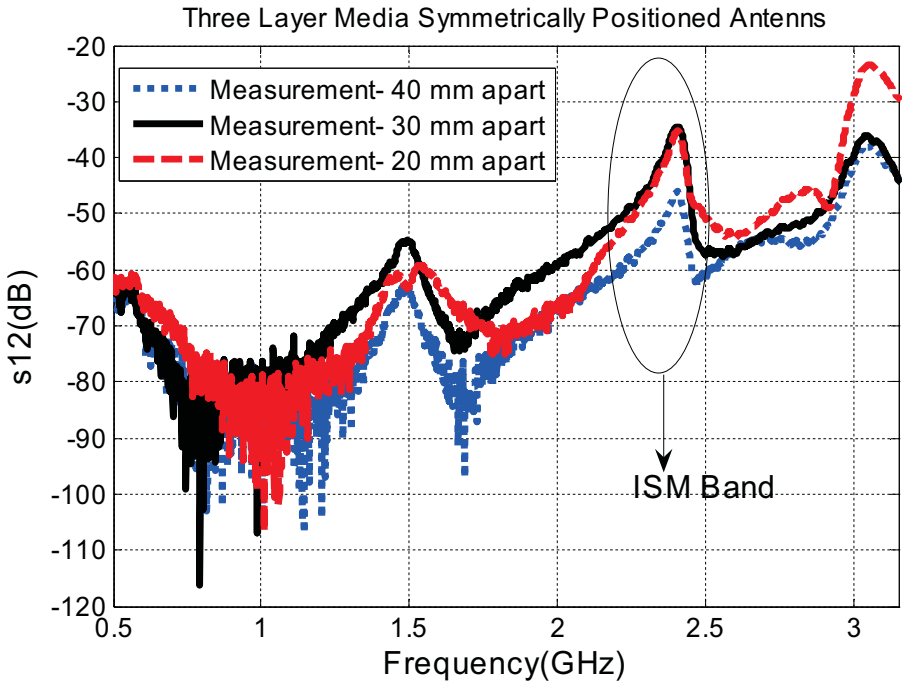

Fig. 3.21 Mutual coupling measurements for antennas mounted 20 mm, 30 mm, and 40 mm apart on three layered tissue mimicking gel covered cardboard

The last set of measurements is taken to investigate the effect of positioning the antennas with different phases according to one another. To do so, the antennas are placed with several different phase differences with respect to each other. It has been concluded that, the least mutual coupling effect can be obtained by placing antennas with a 90 degree phase difference with respect to each other. Fig 3.22 shows two identical ISM band on-body antennas placed on a cardboard with 90 degree phase difference.

The receiver antenna is placed with 90 degree difference with respect to transmitter antenna. The measurements are performed by mounting the on-body antennas on a cardboard, skin mimicking gel covered cardboard, and three layered tissue mimicking gel

covered cardboard. The mutual coupling measurement results are shown in Fig. 3.23, Fig. 3.24, and Fig. 3.25.

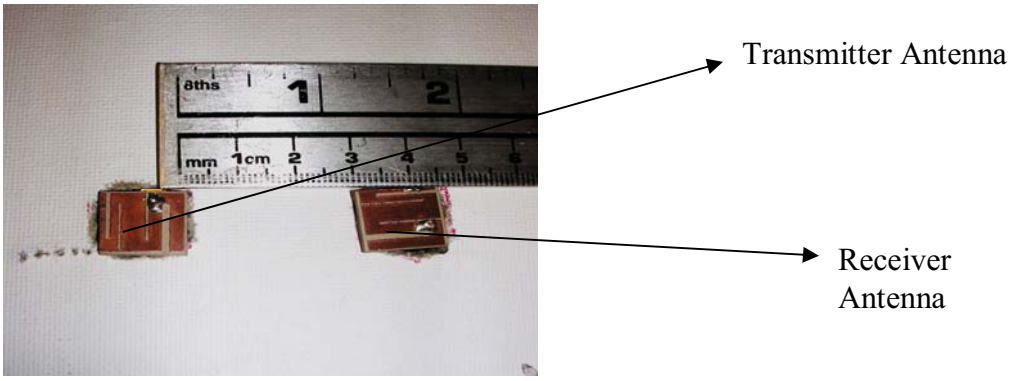

Fig. 3.22 Receiver antenna placed with 90 degree shift with respect to transmitter.

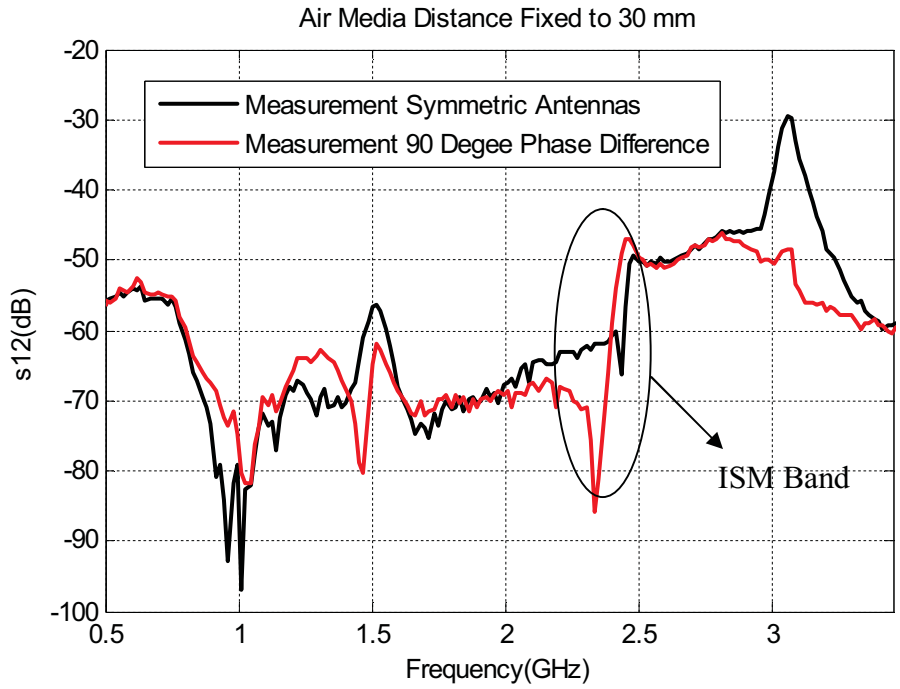

Fig. 3.23 S_{12} comparison of symmetrically placed and 90 degree shifted antennas.

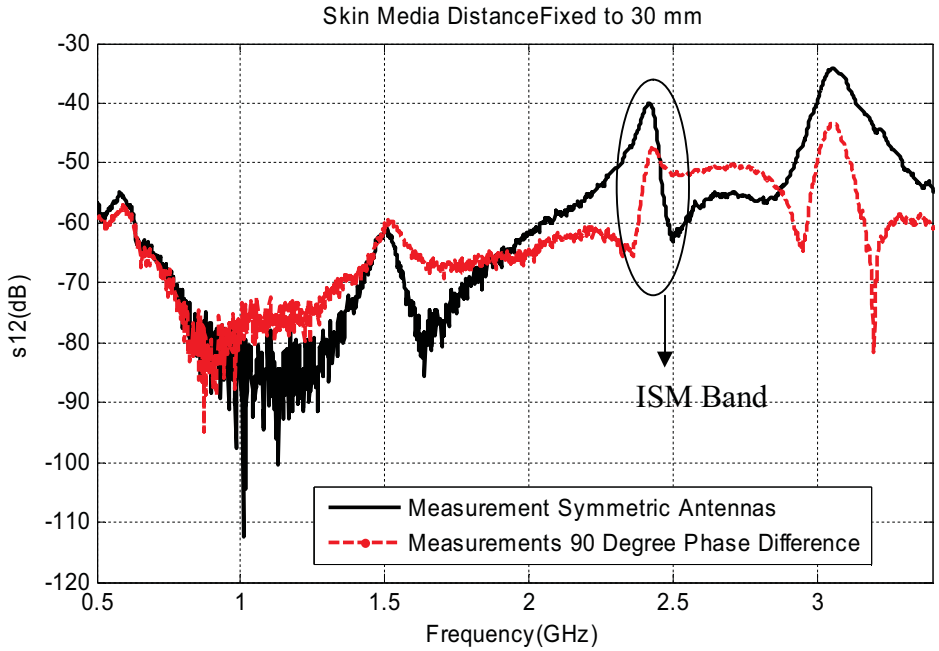

Fig. 3.24 S_{12} comparison of symmetrically placed and 90 degree shifted antennas.

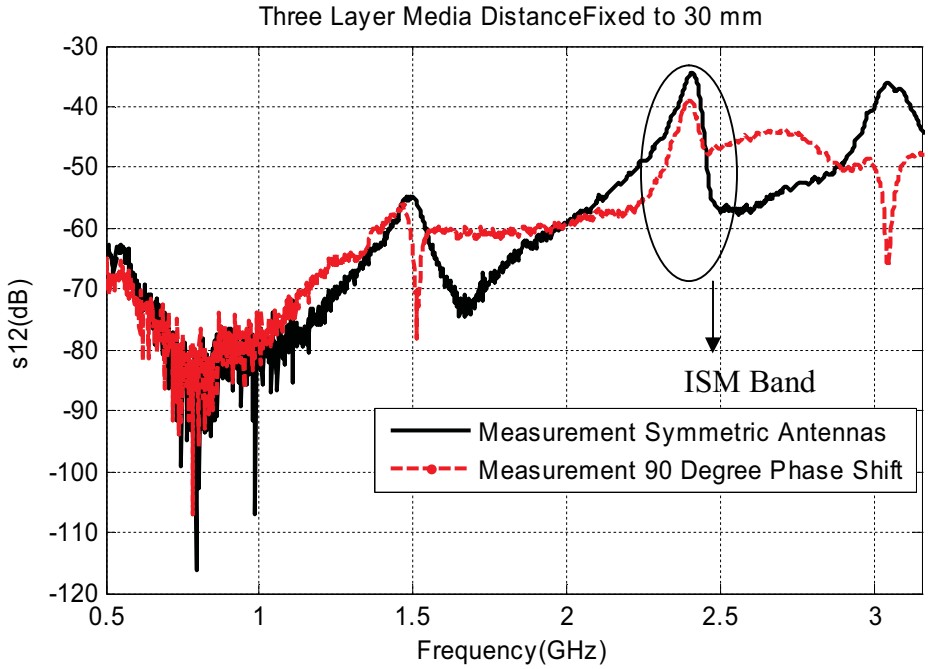

Fig. 3.25 S_{12} comparison of symmetrically placed and 90 degree shifted antennas.

The results are compared with the mutual coupling measurements obtained by placing the antennas symmetrically. Fig. 3.23, 3.23, and 3.23 show the comparisons for a fixed distance of 30 mm. As seen from all figures, shifting the second antenna 90 degree decreases mutual coupling between two antennas approximately 5dB for 2.4 GHz.

CHAPTER IV

CONCLUSION AND FUTURE WORK

4.1 Conclusion

In this thesis, various tissue mimicking materials have been characterized and used to test a dual band implantable antenna and body-centric antennas. The characterized tissue mimicking materials are inexpensive and have simple recipes that are easy to formulate.

A skin mimicking material for ISM Band is developed by using triton X-100, DGBE and distilled water. Testing of a dual band implantable antenna operating at MICS and ISM Bands is performed by embedding the antenna into the skin mimicking material. Since the first developed skin mimicking material is a fluid, a skin mimicking gel for ISM band is characterized by using oil, distilled water, ultra ivory, and agarose. By varying the proportions of ingredients of the skin mimicking gel, a wide band muscle mimicking gel is also obtained. A dual band implantable antenna is tested *in vitro* by placing the antenna between muscle and skin mimicking gels for MICS band [31].

An on-body antenna operating at ISM Band is designed for wireless cardiac monitoring systems and the dimensions of the antenna are optimized by using hybrid PSO-HFSS technique. The antennas are fabricated and mutual coupling measurements are performed. The effect of the tissue layers beneath the antenna to mutual coupling is investigated by placing the antennas on skin mimicking gel covered cardboard and three layered tissue mimicking gel covered cardboard. The effect of the position of the

antennas is also investigated by placing the antennas with various distances and phase differences with respect to one another. Note that all electrical property measurements are performed with Agilent's slim probe kit, and the return loss and mutual coupling measurements are performed with E8362B network analyzer.

A good agreement is obtained for return loss measurements of the implantable antenna. The mutual coupling effect is ignorable for antennas placed more than 40 mm apart. The antennas should be positioned with 90 degree phase difference with respect to one another to minimize the mutual coupling between them. Note that the human torso approximation is a necessity to perform accurate mutual coupling measurements.

4.2 Future Work

Characterization and testing of tissue mimicking materials requires performing many experiments. Obtaining the electrical properties of human tissues is a challenging task that the electrical properties are affected from many factors, and there is no certain algorithm that can be used to predict the changes. During the characterization process the electrical property measurements are carried out trial and error method which is time consuming and costly. To prevent the cost and increase time efficiently, statistical methods should be employed to predict the effect of each ingredient to the electrical properties of the characterized material.

The sensitivity of probes is another common problem on electrical property measurements. Especially, there is a great deal of ambiguity on electrical property

measurements for gel like materials. To obtain accurate measurements, the statistical methods should be applied to investigate the probes sensitivity.

The dual band implantable antenna can be also *in vitro* tested on a three layer structure by placing the antenna between fat and skin mimicking gel layers (see Fig. 4.1). To do so, the bottom of container will be covered with muscle mimicking gel. Then the fat mimicking material will be placed on muscle mimicking gel and the antenna will be mounted on fat mimicking gel. Finally, the antenna and fat mimicking gel will be covered with skin mimicking gel, and the return loss measurements will be performed.

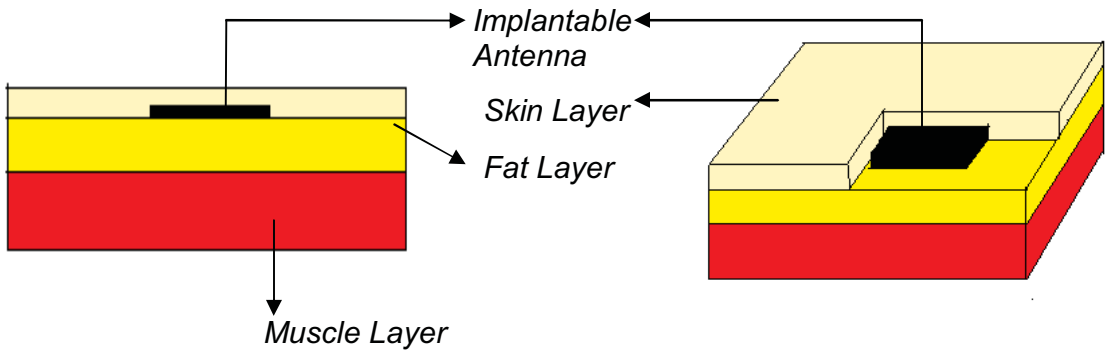

Fig. . 4.1 Return Loss measurement set up.

Mutual coupling measurements of on-body antennas will be performed by covering the surface of a human torso with three layered tissue mimicking material. Antennas with higher bandwidth will be designed. Radiating parts of on-body antennas will be placed toward the human torso to investigate the other effects of positioning to mutual coupling between antennas. Fig. 4.2 shows the measurement set up for mutual coupling measurements

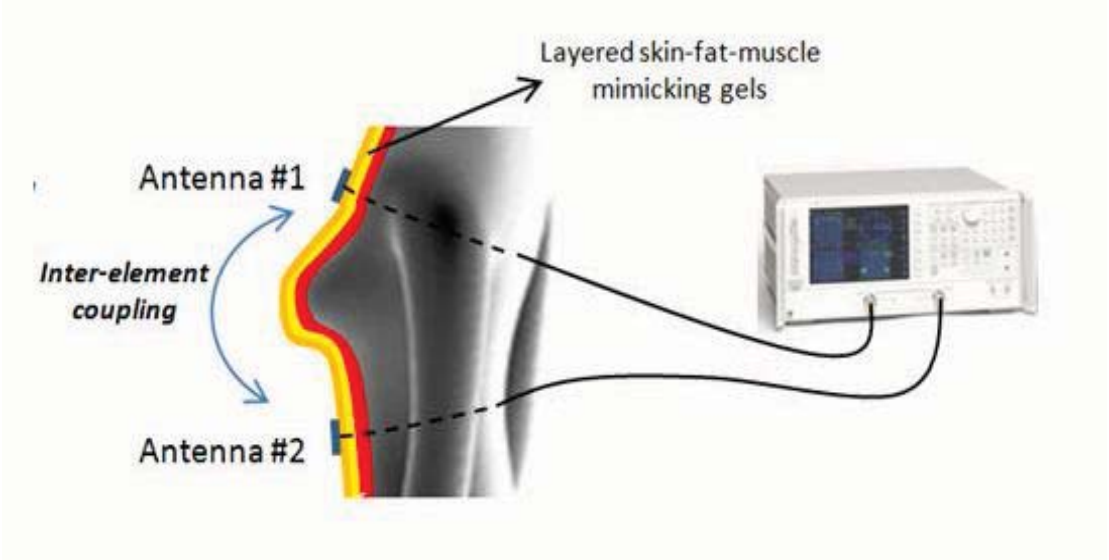

Fig. 4.2 Mutual coupling measurement set up for on-body antennas.

REFERENCES

[1] C. M. Furse, "Design of an antenna for pacemaker communication," *Microwave RF*, vol. 39, no. 3, pp. 73–76, Mar. 2000.

[2] J. Kim and Y. Rahmat-Samii, "Implanted antennas inside a human body: Simulations, designs, and characterizations," *IEEE Trans. Microw. Theory Tech.*, vol. 52, no. 8, pp. 1934–1943, Aug. 2004.

[3] E. Zastrow, S. K. Davis, M. Lazebnik, F. Kelcz, B. D. Van Veen, S. C. Hagness," Development of Anatomically Realistic Numerical Breast Phantoms With Accurate Dielectric Properties for Modeling Microwave Interactions With the Human Breast," *IEEE Transactions on Biomedical Engineering*, vol. 55, no. 12, pp. 2792-2800, December 2008.

[4] C. Gabriel, S. Gabriel, and E. Corthout, "The dielectric properties of biological tissues: I. Literature survey," *Phys. Med. Biol.*, vol. 41, pp. 2231–2249, 1996.

[5] S. Gabriel, R. W. Lau, and C. Gabriel, "The dielectric properties of biological tissues: II. Measurements in the frequency range 10 Hz to 20 GHz," *Phys. Med. Biol.*, vol. 41, pp. 2251–2269, 1996.

[6] D. Gies and Y. Rahmat-Samii, "Particle swarm optimization for reconfigurable phase-differentiated array design," *Microw. Opt. Technol. Lett.*, vol. 38, no. 3, pp. 168–175, Aug. 2003.

[7] K. Fukunaga, S. Watanabe, and Y. Yamanaka "Dielectric Properties of Tissue-Equivalent Liquids and Their Effects on Specific Absorption Rate," IEEE Transactions on Electromagnetic Compatibility, vol. 46, no. 1, pp 126-129, February 2004.

[8] J. Cavuoto, "Neural engineering's image problem," *IEEE Spectr.*, vol.41, no. 4, pp. 32–37, Apr. 2004.

[9] R. F. Weir, P. R. Troyk, G. DeMichele, and T. Kuiken, "Implantable myoelectric sensors (IMES) for upper-extremity prosthesis control," in *Proc. IEEE Eng. Med. Biol. Soc 25th Annu. Int. Conf.*, Sep. 2003, pp. 1562–1565.

[10] R. D. Beach, R. W. Conlan, M. C. Godwin, and F. Moussy, "Towards a miniature implantable *in vivo* telemetry monitoring system dynamically configurable as a potentiostat or galvanostat for two- and threeelectrode biosensors," *IEEE Trans. Instrum. Meas.*, vol. 54, no. 1, pp. 61–72, Feb. 2005.

[11] D.M. Pozar, "Microstrip antennas," Proceedıngs of the IEEE, vol. 80, no. 1, pp 79-91, January 1992.

[12] D.H. Schaubert, D.M. Pozar, A. Adrian, "Effect of microstrip antenna substrate thickness and permittivity: comparison of theories with experiment," *IEEE Transactions on Antennas and Propagatıon*, vol. 37**,** no. 4**,** April 1989.

[13] D.M. Pozar, B.Kaufman, "Design considerations for low sidelobe microstrip arrays,**"** *IEEE Transactions Antennas and Propagation,* vol. 38, Issue 8 pp.1176 – 1185, Aug. 1990.

[14] D.M. Pozar, B.Kaufman, "Increasing the bandwidth of a microstrip antenna by proximity coupling,**"** *IEEE Electronics Letters*, vol. 23, Issue 8, pp. 368 – 369, April 9 1987.

[15] J. R. James and P. S. Hall, *Handbook of Microstrip Antennas*, ser. IEEE Electromagnetic Waves. London, U.K.: Peter Peregrinus, 1989, vol. 28.

[16] T. Karacolak E. Topsakal, "A Double-Sided Rounded Bow-Tie Antenna (DSRBA) for UWB Communication*," IEEE Antennas and Wıreless Propagation Letters*, vol. 5, pp. 446-449, 2006.

[17] J. Robinson and Y. Rahmat-Samii, "Particle swarm optimization in electromagnetics," *IEEE Trans. Antennas Propag.*, vol. 52, no. 2, pp. 397–407, Feb.2004.

[18] S. Xu, Y. Rahmat-Samii, and D. Gies, "Shaped-reflector antenna designs using particle swarm optimization: An example of a direct-broadcast satellite antenna," *Microw. Opt. Technol. Lett.*, vol. 48, no. 7, pp. 1341–1347, Jul. 2006.

[19] D. Gies and Y. Rahmat-Samii, "Particle swarm optimization for reconfigurable phase-differentiated array design," *Microw. Opt. Technol. Lett.*, vol. 38, no. 3, pp. 168–175, Aug. 2003.

[20] J. Kennedy and R. Eberhart, "Particle swarm optimization," in *Proc. Int. Neural Networks Conf.*, Perth, Australia, 1995, vol. IV, pp. 1942–1948.

[21] N. Jin and Y. Rahmat-Samii, "Parallel particle swarm optimization and finite-difference time-domain (PSO/FDTD) algorithm for multiband and wideband patch antenna designs," *IEEE Trans. Antennas Propag.*, vol. 53, no. 11, pp. 3459–3468, Nov. 2005.

[22] A.Z. Hood, E. Topsakal, **"**Particle swarm optimization for dual-band implantable antennas**,"**Antennas and Propagation International Symposium, June 2007 pp. 3209 - 3212 ,2007.

[23] T. Karacolak, A. Z. Hood and E. Topsakal," Design of a Dual-Band Implantable Antenna and Development of Skin Mimicking Gels for Continuous Glucose Monitoring," *IEEE Transactions on Microwave Theory and Techniques,* vol. 56, no. 4, pp. 1001-1008, April 2009.

[24] A. Alomainy, Y. Hao, X. Hu, C.G. Parini, and P.S. Hall, "UWB on-body radio propagation and system modelling for wireless body-centric networks," IEE Proc., Commun., vol.153, no.1, pp.107–114, Feb. 2006.

[25] A. Alomainy, Y. Hao, A. Owadally, C.G. Parini, Y. Nechayev, C.C. Constantinou, and P.S. Hall, "Statistical analysis and performance evaluation for on-body radio propagation with microstrip patch antennas," IEEE Trans. Antennas Propag., vol.55, no.1, pp.245–248, Jan. 2007.

[26] D. Psychoudakis, C.-C. Chen, and J.L. Volakis, "Wearable antenna optimization and fabrication for VHF/UHF applications," URSI North American Radio Science Meeting, Ottawa, Canada, 2007.

[27] P.S Hall, "Antennas and propagation for body centric communications," *IET Seminar*, pp.1 – 4, 24 April 2007.

[28] P.S. Hall, "Antennas Challenges for Body Centric Communications,**"** *IWAT '07. International Workshop*, pp. 41 – 44, 21-23 March 2007.

[29] S.M Pitchers, D.A Eves, "A protocol for body centric networks," *IEE Eurowearable* pp. 87 - 92, Sept. 2003.

[30] M Lazebnik, E. L. Madsen, G. R. Frank, and S. C. Hagness, "Tissue-mimicking phantom materials for narrowband and ultrawideband microwave applications," *Physics in Medicine and Biology*, vol. 50, pp. 4245-4258, 2005.

[31] "Medical implant communications service (MICS) federal register," *Rules Reg.*, vol. 64, no. 240, pp. 69926–69934, Dec. 1999.